

Recent Developments on Flexible Materials for Thermoelectrics

Mohammedhamidraza A Mawazzan, Anita B. Padasalagi, B. Manoj*, and M. K. Rabinal[†]

Abstract

In recent decades, thermoelectric materials have gained a significant attention due to their ability to directly convert waste heat into electricity. While extensive research has been focused on enhancing the thermoelectric properties of inorganic bulk materials, a new frontier has emerged in this area as flexible thermoelectric materials. These flexible thermoelectrics are driven by the limitations posed by the rigidity, less functional and toxicity of conventional inorganic thermoelectric materials. Despite notable achievements in the development of high-performance flexible thermoelectric materials, they still pose inferior figure of merit (zT) in comparison to their inorganic counterparts. This review encompasses various aspects of flexible thermoelectric materials including theoretical foundations which highlight the principles that explain the concepts and parameters of thermoelectricity to enhance the overall performance, serving as a foundation for understanding the subsequent developments. Further it is overviewed in detail the corresponding state of the art in development of conducting thermoelectric polymers, inorganic-polymer composites, carbon-based thermoelectric and inorganic thermoelectrics on flexible substrates to enhance their thermoelectric performances. Finally, it includes the overlook to the future of flexible thermoelectric for wearable thermoelectrics.

* Dept. of Physics and Electronics, CHRIST (Deemed to be University), Bengaluru, 560029, Karnataka, India Corresponding Author: mkrabinal@yahoo.com

† Dept. of Physics, Karnatak University, Dharwad - 580003, Karnataka, India

Keywords: Flexible thermoelectrics; Figure of merit; Seebeck coefficient; nanocomposites; organic polymers.

Introduction

The global reliance on fossil fuels for energy production has led to an alarming energy crisis, characterized by wastage and inefficiency in energy consumption. As per the statistics, only approximately 34% of the energy produced through fossil fuel combustion is utilized efficiently, with the remaining untapped portion dissipating into the environment as a waste heat [1]. This inefficiency is not only environmentally disastrous but also economically unsustainable. One best example of energy wastage can be found in petrol-driven vehicles, hardly 25% of the energy is derived from fuel combustion contributes to vehicle mobility and accessories. The rest, a substantial 75%, is lost in the form of waste heat [96]. Similarly, in power plants, steel and iron factories, car engines, and everyday electronics, 60% of the energy generated by fossil fuels worldwide is wasted as heat. Moreover, significant proportion of this untapped energy is in the form of low-heat below 100 °C, which accounts for 42% of all wasted energy. Additionally, waste heat falling within the range of 100 °C to 200 °C contributes 22% of the energy lost [2]. This wastage of resources highlights the urgency of addressing the global energy crisis. Moreover, it emphasizes the necessity of not only improving overall energy conversion efficiency but also developing innovative technologies to harness and repurpose this lower-grade waste heat.

Thermoelectric (TE) materials present a promising solution to address these challenges of converting low-grade waste heat into useful electrical power, operating on a phenomenon known as the Seebeck effect [98]. The principle behind thermoelectric energy harvesting involves the movement of charge carriers (electrons for n-type materials and holes for p-type materials) from the hot side to the cold side when a temperature difference (ΔT) is applied. This movement generates an electrostatic potential (ΔV), essentially creating a voltage difference [3]. One of the notable advantages of this technology is its silent and reliable operation, as it doesn't involve any moving parts [1]. Interestingly, the concept of using thermoelectric techniques for energy generation has roots dating back to the 1960s, when it

was employed to power deep space satellites engaged in long-term explorations. More recently, beginning in the late 20th century, the application of thermoelectric principles has expanded due to pressing concerns such as the energy crisis and intensified greenhouse gas emissions. This expansion has led to the adaptation of thermoelectric methods for the purpose of harvesting waste heat, conversion of lost energy into useful electricity [4]. The electrostatic potential produced by a single thermoelectric device (TED) is quite minimal, ranging from a few microvolts to millivolts depending on the context. To achieve substantial output voltage and power, thermoelectric generators (TEG) are typically constructed using multiple TE couples, often dozens or even hundreds of them in series.

Existing commercially employed thermoelectric materials contain substantial quantities of rare elements like tellurium or lead (found in stoichiometric compounds such as Bi_2Te_3 , PbTe etc.), boosting the figure of merit (zT). Generally, figure of merit is referred as the dimensionless quantity which signifies the efficiency of thermoelectric generator. However, these pose a barrier to future scaling up due to less abundant, heavy and toxic elements. While conventional rigid TE materials have shown considerable progress, there is a growing demand for flexible and conformable thermoelectric devices to address emerging applications. Flexible thermoelectric (FTE) offer a convenience in the design and implementation of energy conversion systems. Unlike their rigid counterparts, these materials can conform to complex shapes, adhere to irregular surfaces, and withstand mechanical deformations without compromising their electrical and thermal properties. This flexibility opens up a wide range of possibilities for integrating thermoelectric technology into previously untapped areas, such as wearable electronics, devices, medical implants, and even smart fabrics. To maximize the thermoelectric efficiency, several novel strategies have been explored including, engineering the nanostructures and composition of these materials to overcome the bottleneck for thermoelectrics in maintaining a delicate balance between electrical conductivity, Seebeck coefficient and thermal conductivity, which deduce the figure of merit.

1. Overview of Thermoelectrics

The origin of thermoelectricity can be traced back to the early 19th century when scientists like **Thomas Seebeck** and **Jean Peltier** discovered the phenomenon of thermoelectric effects. In 1821, **Seebeck** found that when two different metals were connected in a closed circuit, in which one junction was heated while the other was cooled, the magnetic needle near to the circuit deflects [3]. Initially, it was believed that deflection in magnetic needle is due to earth’s magnetic field but later it was realized that an electric current in the circuit is being generated as a function of temperature gradient in direct proportion. The phenomenon is popularly known as “Seebeck Effect” and the proportionality constant between the temperature gradient and electric voltage generated per unit temperature gradient is called Seebeck Coefficient (S), which is given as.

$$S = - \left(\frac{\Delta V}{\Delta T} \right) \text{-----} (1)$$

The understanding of the Seebeck effect, coupled with the progressing theories of electromagnetism, sparked a chain of investigations into the transformation of heat into electrical current and vice-versa. In 1834, **Jean Charles Athanase Peltier**, discovered that the junction of two dissimilar metals would experience heating or cooling when subjected to an electrical current [5]. This was the exact complimentary phenomenon of Seebeck effect. In 1838, **Lenz** demonstrated that the direction of the current flow determines whether the junction would absorb heat (resulting in the water to freeze into ice), or generate heat (for ice melting), upon reversing the current [6]. The amount of heat absorbed or liberated at the junction (dQ/dt) is directly proportional to the electrical current (I), where Q is the heat energy. This proportionality is characterized by the Peltier coefficient (P) which is given by

$$\frac{dQ}{dt} = PI \text{-----} (2)$$

The Peltier coefficient also can be expressed as the product of the Seebeck coefficient (S) and the absolute temperature (T).

$$P = TS \text{-----} (3)$$

In 1851, **Heinrich Gustav Magnus** made a significant discovery that the Seebeck voltage is not a function of temperature distribution across the metals, but rather it explicitly depend on temperature gradient between the junctions [6]. This revelation served as a mile stone for the explanation to Seebeck coefficient as a thermodynamic state function. Further, **William Thomson (Lord Kelvin)** advanced the understanding of thermoelectricity with his work on the Thomson effect in the 1850 [3]. When an electric current flowed through a conductor kept at temperature gradient, either absorbed heat (cooling effect) or released heat (heating effect) depending on the direction of the current and temperature gradient. The rate of change in heat is directly proportional to the current (I) and the temperature gradient (dT) within the length element (dx). Where the proportionality constant (τ) is called Thomson’s coefficient which can be expressed as

$$\frac{d}{dt} \left(\frac{dQ}{dt} \right) = \tau I \left(\frac{dT}{dx} \right) \text{----- (4)}$$

Figure (1) representing the schematic illustration of (a) Seebeck, (b) Peltier and (c) Thomson effects. These discoveries attracted the attention of scientific community to study the interconversion of thermal and electrical energies. In 1885, the British physicist **John William Strutt Rayleigh** proposed the utilization of the Seebeck effect for power generation [6]. Although he initially failed to accomplish the satisfactory results but it can be regarded as the foundation of the concept of converting thermal energy into electrical energy. Later many more attempts were made to get an efficient thermoelectric generator by connecting number of conductors electrically in series and thermally in parallel, employing hot gases or liquids as heat sources. Among all other attempts the Clammond pile, madeup of 3000 thermocouples gained considerable attention which was able to generate 109 V with maximum output power of 200 W which is nearly equal to 10 Kg coal burnt per hour [6].

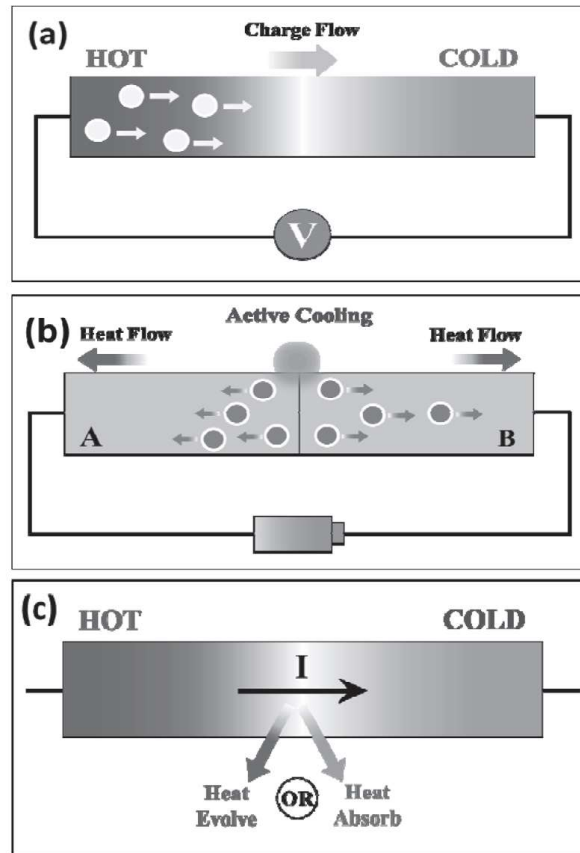


Figure 1: Schematic representation of (a) Seebeck effect, (b) Peltier effect, and (c) Thomson effect

Next, **Edmund Altenkirch**, a German physicist, made a significant contribution to the field of thermoelectricity. In 1909, he achieved a notable milestone by deriving the maximum efficiency (denoted as η) of a thermoelectric generator [6-7]. This efficiency represents the ratio of electric power generated by the generator to the heat supplied at its hot side over a unit of time. His work revealed that the efficiency of thermoelectric conversion is directly proportional to the efficiency of Carnot's cycle, which serves as an upper limit for thermoelectric processes. Additionally, **Altenkirch** identified crucial material properties that dictate the thermoelectric performance of these materials. One of his significant findings was that effective thermoelectric devices should utilize thermocouples with several key characteristics. These characteristics include large Seebeck coefficient, which indicate the magnitude of the thermoelectric effect, low electrical resistance, and minimal thermal conductance.

These properties collectively contribute to enhancing the overall performance of thermoelectric engines by facilitating efficient conversion of heat into electricity [3,7]. Further, the Russian physicist **Abram Fedorovich Loffe** began to formulate the modern theory of semiconductor physics. In 1949, while modeling the conversion efficiency of thermoelectric devices under the approximation of temperature-independent thermoelectric properties, he introduced for the first time the dimensionless thermocouple figure of merit (zT) given by [3,8]

$$zT = \frac{S^2\sigma T}{\kappa} \text{ --- (5)}$$

The term $S^2\sigma$ is referred as power factor, where S is Seebeck coefficient, σ is electrical conductivity, T is temperature and κ is thermal conductivity. The bottle neck for better figure of merit lies in maintaining this delicate balance of high Seebeck coefficient, high electrical conductivity and lower thermal conductivity, the dependence of these parameters on carrier concentration are shown in **Figure (2)**.

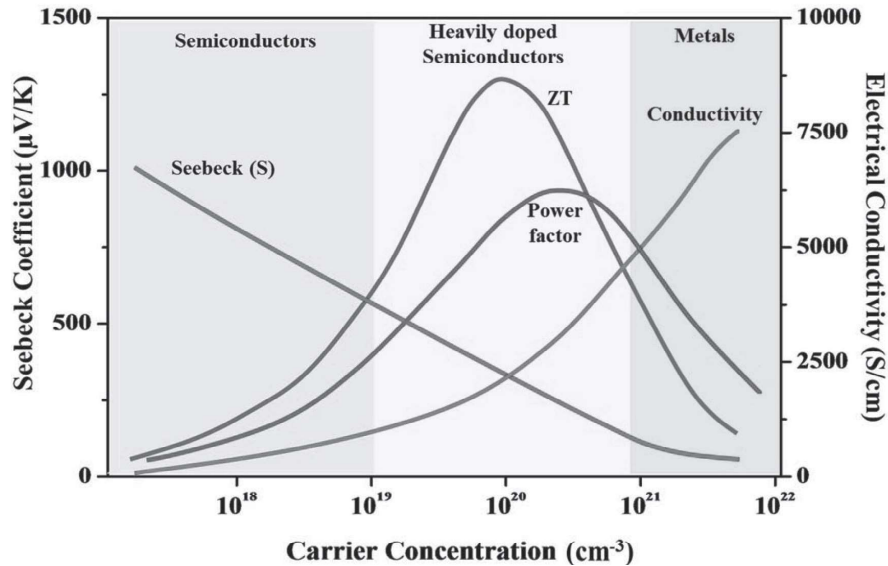


Figure 2: Representation of relationship between Seebeck coefficient, electrical conductivity, power factor and figure of merit as a function of carrier concentration

Further, the continuous progress in semiconductor research led to productive thermoelectrics with considerable improvement in the efficiency. Profoundly in 1947, **Maria Telkes** developed a thermoelectric generator using PbS and ZnSb. This generator achieved a conversion efficiency of over 5% when operated across a 400 K temperature difference [3,6,9]. In 1954, **Hiroshi Julian Goldsmid** demonstrated cooling at 273K using a Bi₂Te₃ thermocouple-based thermoelectric device. During the 1950s, the Soviet Union introduced ring-shaped thermoelectric generators consisting of ZnSb/Constantan thermocouples. These generators were used to convert heat from kerosene lamps and power radio receivers in rural areas without direct access to electricity. In the pursuit of improving thermoelectric generator efficiency, interest grew over the years. In the 1990s, **Glen Slack** introduced a groundbreaking concept known as the "Phonon Glass-Electron-Crystal" (PGEC). This innovative idea aimed to separate the electrical and thermal conductivities within the same material, otherwise these parameters are directly related to carrier density of a material ($\sigma = ne\mu$ and $L_0\sigma T(\frac{k_B}{e})^2$), increasing σ also increases k and hence reduce the zT . Slack's concept suggested that phonons, which carry heat, could be controlled similarly to how they behave in a glass (highly localized), while electrons could flow freely as they do in a crystalline conductor (highly delocalized) [10]. Further **Hicks and Dresselhaus's** theoretical investigations highlighted the potential for decoupling of electron and phonon conductivity in nanomaterials, offering new opportunities for enhancing thermoelectric efficiency and effectiveness [6]. These concepts served as significant step in the field of TE towards the enhancement of figure of merit (zT) offering an innovative approach towards fabrication.

The efficiency (η) of a thermoelectric device can be calculated through the application of thermodynamic principles, specifically energy conservation between the high temperature (T_h) and low temperature (T_c) of the material. This efficiency is influenced by two main factors: the Carnot efficiency (η_c) and the dimensionless figure of merit (zT) as given below

$$\eta = \eta_c f(zT) \text{----- (6)}$$

where the Carnot efficiency η_c and $f(zT)$ are respectively given by

$$\eta_c = \frac{T_h - T_c}{T_h}, f(zT) = \frac{\sqrt{1 + zT} - 1}{\sqrt{1 + zT} + \left(\frac{T_c}{T_h}\right)} \text{----- (7)}$$

This visualizes the compulsion of high zT for superior efficiency of thermoelectric engine. In semiconductors, the Seebeck coefficient typically decreases as the concentration of free charge carriers (electrons or holes) increases. This phenomenon has been firmly established through experimental observations, particularly in TE as shown in Figure (2). The Mott-Boltzmann formalism explains this phenomenon by considering energy-independent scattering of charge carriers. The predicted Seebeck coefficient as per the theory, applicable to both metals and degenerate semiconductors featuring a parabolic band structure and energy-independent scattering of charge carriers, further it implicitly depends upon the carrier concentration (n), as well as the effective mass (m^*) given by [11-12]

$$S = \frac{8\pi^2 k_B^2 T}{3eh^2} m^* \left(\frac{\pi}{3n}\right)^{\frac{2}{3}} \text{----- (8)}$$

where k_B and h are Boltzmann constant and Planck’s constant, respectively.

Further it can be noted that the electrons in the lattice are treated in accordance to the free electron model and characterized by effective mass m_e^* . If τ_e and e are the collision mean time and electric charge of the conduction electron respectively, then the electrical conductivity is given by

$$\sigma_e = ne\mu_e = \frac{ne^2\tau_e}{m_e^*} \text{----- (9)}$$

here, μ_e is the mobility of electron. It can be noted from equation (8) and equation (9) that, for a given semiconductor. It can be noted that electrical conductivity is directly proportional to carrier concentration, whereas the Seebeck coefficient is inversely related

to carrier concentration. Hence the increase in carrier concentration promotes the electrical conductivity but adversely affects the Seebeck coefficient. Moreover, another dominant parameter which governs the value of zT is thermal conductivity (κ). Thermal conductivity in conductors is signified by two types i.e. thermal conductivity due to electrons (κ_e) and phonons (κ_{ph}) which are also known as carrier thermal conductivity and lattice thermal conductivity respectively.

$$\kappa = \kappa_e + \kappa_{ph} \text{ --- --- --- --- --- --- --- --- --- --- (10)}$$

According to the Wiedemann–Franz law κ_e is in direct proportion to the electrical conductivity which is quantitatively given as

$$\kappa_e = L_0 \sigma T \left(\frac{k_B}{e} \right)^2 \text{ --- --- --- --- --- --- --- --- --- --- (11)}$$

where k_b is Boltzmann constant, e is electron charge, L_0 is a dimensionless constant which is equal to $(\pi^2/3)$ for metallic conductors and equals to 2 for semiconducting systems as proposed by Maxwell-Boltzmann statistics [3,18]. The linear relationship between electrical conductivity (σ) and carrier thermal conductivity(κ_e), as dictated by the Wiedemann–Franz law in equation (11), raises concerns about very high electronic conductivities (exceeding 2000-3000 Scm⁻¹ at room temperature). Such extreme conductivities might be a significant obstacle for their implications. For illustration, consider n-type PbTe who’s the total thermal conductivity is 1.3 Wm⁻¹K⁻¹ at 700 K. In optimized samples of this material, approximately 0.15 Wm⁻¹K⁻¹ can be attributed to κ_e , arising from an electronic conductivity of around 200 Scm⁻¹ at 700 K. Consequently, a rise in electronic conductivity by 200 Scm⁻¹ results in an additional thermal conductivity of 0.15 Wm⁻¹K⁻¹ at the same temperature. This situation imposes significant limitations on the permissible lattice thermal conductivity to achieve a high zT value. Therefore, the only effective way to enhance the zT is to minimize lattice thermal conductivity (also known as phonon thermal conductivity, κ_{ph}). As approximated by classical kinetic theory, the lattice thermal conductivity is given by the following equation

$$\kappa_{ph} = \frac{C_v l v_s}{3} \text{ --- --- --- --- --- --- --- --- --- --- (12)}$$

where C_v is the specific heat capacity at constant volume, v_s is the mean velocity of sound wave and l is the mean free path of phonon [13]. At very low temperatures adjacent to 40 K, the number of excited phonons is insignificant and they possess a longer wavelength. At lower temperatures κ_{ph} is governed by Debye's T^3 law for C_v , hence the lattice thermal conductivity is negligible. However above Debye temperature, the value of C_v reaches the classical limit of $3R$ and κ_{ph} gets dominated by l . Here the lattice thermal conductivity κ_{ph} is primarily dominated by phonon-phonon scattering in accordance with Keyes's equation [14]

$$\kappa_{ph}T = \frac{R^{3/2} T_m^{3/2} \rho^{2/3}}{3\gamma^2 \epsilon^3 N_0^{1/3} A^{7/6}} \text{ --- (13)}$$

where T is the temperature, R is the ideal gas constant, T_m is the melting point, ρ is the density, γ is the Gruneisen constant, ϵ is the fractional amplitude of inter atomic thermal vibration, N_0 is the Avogadro number and A is the mean atomic weight. This law concludes the four important outcomes on thermal conductivity: (a) At elevated temperatures, lattice thermal conductivity is in inverse proportionality with temperature, (b) lattice thermal conductivity is lower for larger atomic weights, (c) lower melting points directs to lower lattice thermal conductivity and (d) larger atomic distance leads to lower density which intern induce the lower lattice thermal conductivity. These significant milestones in advancement of thermoelectric research is depicted in **Figure (3)**.

An effective method to diminish lattice thermal conductivity and intern enhance the zT value has involved modifying to already promising compounds through the introduction of point defects in the lattice. A classic illustration of this strategy is Bi_2Te_3 system, within this $\text{Bi}_{2-x}\text{Sb}_x\text{Te}_3$ and $\text{Bi}_2\text{Te}_{3-x}\text{Se}_x$ have demonstrated superiority over the parent compound. This refinement primarily arises from reduction in thermal conductivity. For instance, the thermal conductivity of the solid solution is notably lower at $1.5 \text{ Wm}^{-1}\text{K}^{-1}$ compared to the parent compound's $2.4 \text{ Wm}^{-1}\text{K}^{-1}$ [14]. This decrease in thermal conductivity reflects as enhancement of the zT value at room temperature in the order of unity. In contrast, the parent Bi_2Te_3 compound achieves value of around 0.6 [14-15]. Furthermore, other highly effective strategies

focus on exploiting boundary scattering as a means to substantially diminish lattice thermal conductivity to impressively low levels. One appealing approach includes the grinding of a material followed by its compression into a pellet using techniques such as hot pressing or spark plasma sintering [16-17].

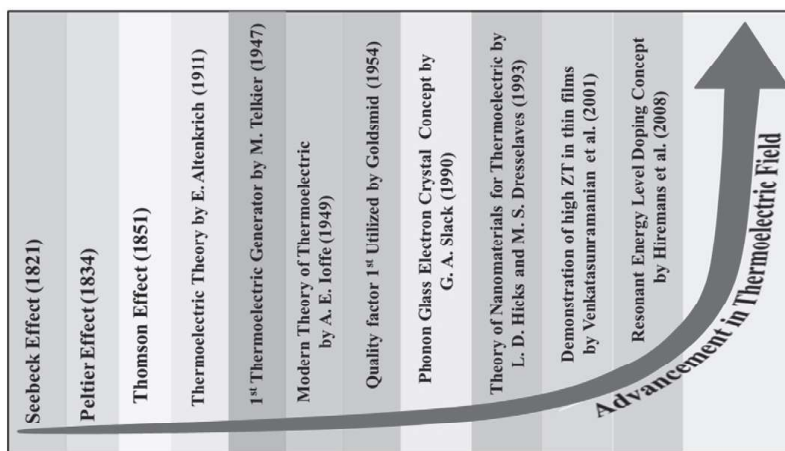


Figure 3: Representation of important milestones and advancements in thermoelectric field.

Over the years, significant enhancements have been observed in the field of thermoelectric, leading to optimization of thermoelectric systems for efficient thermoelectric conversion. Moreover, the inorganic candidates like skutterudites, clathrates, Zintl compounds, half-Heusler alloys, and metal dichalcogenides are known to showcase impressive zT values. However, conventional inorganic thermoelectric materials such as Bi_2Te_3 , SnSe , SiGe , PbTe , and GeTe suffer with inherent limitations like high costs, involvement of toxic elements, excessive thermal conductivity and processing complexities etc. In contrast, there has been emerging interest in exploring alternative materials like oxides and organic compounds to overcome these challenges. Some oxides such as SrTiO_3 , $\text{Ca}_3\text{Co}_4\text{O}_9$, BiCuSeO , and Bi_2O_2 are abundantly available with robust thermal and chemical stability [18]. Despite these merits, their thermoelectric performance yet to overcome that of conventional counterparts. Currently, in order to establish the extensive use of TEGs for waste heat recovery technology, there are significant scientific challenges that need to be addressed among which development of practical methods to fabricate flexible and shape-engineerable materials is of

great concern. In this respect, next section will be mainly focused on the recent development of flexible thermoelectric in detail.

2. Flexible Thermoelectrics

Traditional TE materials and devices are mainly made of mould, irregular semiconductor materials, which are toxic, heavy, brittle, and rigid. Owing to this non-flexible nature it is difficult to attach over the non-flat/non-uniform surface. In order to tackle these obstacles, presently, great efforts have been put in the field of flexible thermoelectric materials/devices [18]. The light and flexible nature of these TE materials can minimize the loss of thermal energy and achieve the better efficiency of energy conversion by making close contact with any shape of heat source or hot surface. Alongside, they can sustain consistent performance under various deformations such as folding, stretching, pressing, bending and even twisting. It is well noticed that, recently, among the various application fields, energy harvesting through FTEs can be customized to variety of curved/non uniform heat sources like circular tubes, surface, and human body. Such advantages can drive low power consumption electronic devices, and exploring as one of the most acknowledged technologies in the development of self-powered systems. Because of these desirable merits, FTE materials gained a considerable momentum in the renewable energy and low temperature waste thermal energy conversion, which is evidenced from the number of publications for the last ten year as shown in **Figure (4)**.

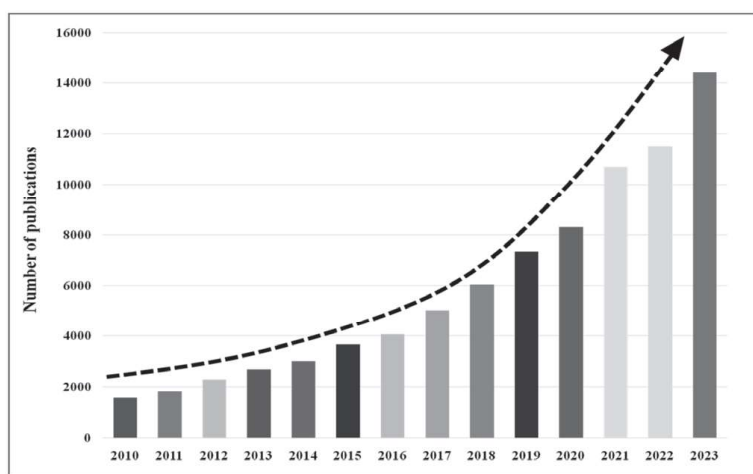


Figure 4: Graphical presentation of progress in flexible thermoelectric research from the year 2010 to 2023.

3. Types of Flexible Thermoelectric Materials and their Devices

To achieve performance requirements for flexible TE devices, selection of thermoelectric material is an important aspect to investigate. However, incapability of bulk TE materials to tie tightly over hot surface lacks their use in emerging flexible electronics. On other hand, well known thermoelectric material suffering from obstacles such as toxicity, expensive, high thermal conductivity and requirement of complicated steps in synthesis limits their potential applications particularly in biomedical field and wearable electronics. Therefore, development of low cost, biocompatible, easy synthesis and eco-friendly flexible thermoelectric materials is highly needed. To bridge over the requirements, organic thermoelectric polymers and their nanocomposites can be a considerable option. The inherent flexibility, reduced weight, and low thermal conductivity ($0.1-0.8 \text{ Wm}^{-1}\text{K}^{-1}$) of organic polymer materials position them as a promising alternative to their inorganic counterparts [19-20]. The potential of organic conducting polymers such as polyphenylenevinylene (PPV), polythiophene (PTH), polyacetylene (PA), polyaniline (PANI), polypyrrole (PPY), polycarbazoles (PC), poly(3,4-ethylenedioxythiophene): poly(styrenesulfonate) (PEDOT:PSS) and their derivatives, are highlighted by their low density, cost-effectiveness, and versatile processing. At same time, better thermoelectric efficiency, may be accomplished in inorganic-polymer composite materials. For instance, in case of inorganic/organic hybrid material, the high Seebeck coefficient and electrical conductivity of the inorganic constituents can be integrated with the poor thermal conductivity of the organic materials and hence enhances thermoelectric efficiency. Therefore, considering all these in account, in the next section, we highlight the conducting thermoelectric polymers, inorganic nanocomposites, carbon-based nanocomposites and other flexible thermoelectrics with current state-of art strategies to optimize the their thermoelectric characteristics. **Figure (5)** highlight the summery of this review.

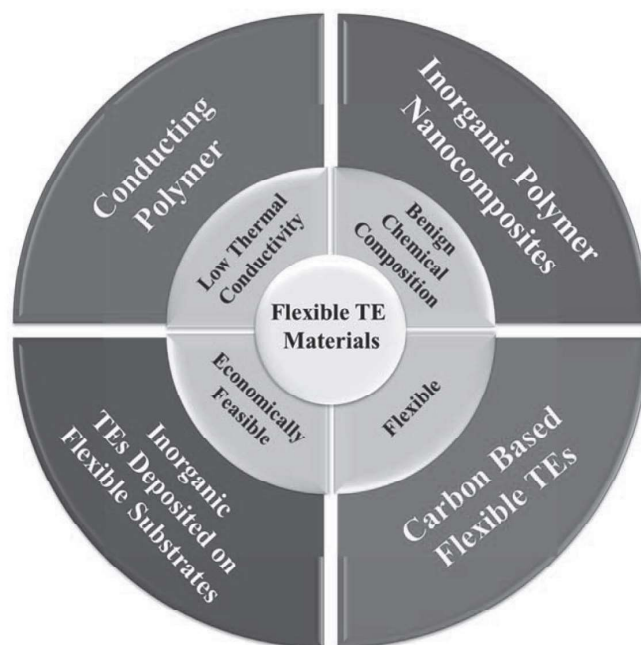


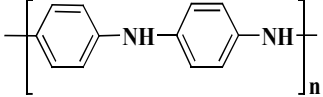
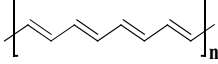
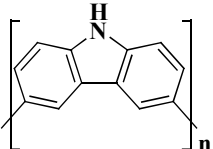
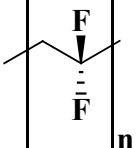
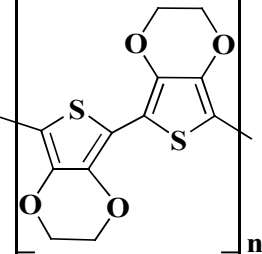
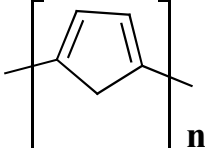
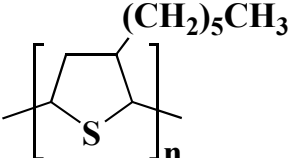
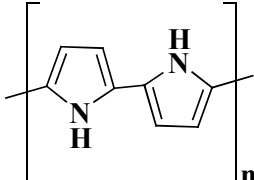
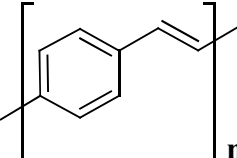
Figure 5: Schematic representation summarizing the main content of this review i.e. recently emerging advanced materials for flexible thermoelectric.

4.1. Conducting Polymer Thermoelectrics

In the 1970s, conducting polyacetylene (PA) was first discovered by Alan Heeger, Alan MacDiarmid, and Hideki Shirakawa, leading to their joint Nobel Prize in 2000 in chemistry. This breakthrough made the way for the exploration of various conducting polymers [21]. These polymers, particularly π -conjugated polymers, constitute a significant category of organic TE materials. These materials derive their thermoelectric properties from the π -conjugated systems present in their chemical structure. Within these systems, the atom's delocalized π -orbital electrons give rise to molecular π -orbital. Consequently, these delocalized electrons highlight the electronic characteristics of these polymers. The doping processes inherent to p and n-type behavior in conjugated polymers are achieved by respectively introducing and removing electrons through oxidation and reduction reactions [22-23]. Several conducting polymers find application in the fabrication of organic TE devices. These include: Poly(3-hexylthiophene), Polyvinylidene fluoride, Polycarbazoles, Polyacetylene, Poly(aniline), Polypyrrole, Polythiophenes, Polyphenylenevinylene, and Poly(3,4-ethylenedioxythiophene). The structure of these polymers are given

in **Table (1)**. Among these few are discussed below in accordance with their thermoelectric properties and their derivatives.

Table 1: Structure of some important conducting polymers

 <p style="text-align: center;">Polyaniline</p>	 <p style="text-align: center;">Polyacetylene</p>	 <p style="text-align: center;">Polycarbazole</p>
 <p style="text-align: center;">Polyvinylidene fluoride</p>	 <p style="text-align: center;">Poly(3,4-ethylene dioxothiophene)</p>	 <p style="text-align: center;">Polythiophene</p>
 <p style="text-align: center;">Poly(3-hexylthiophene)</p>	 <p style="text-align: center;">Polypyrrole</p>	 <p style="text-align: center;">Polyphenylene venvylene</p>

4.1.1. Poly(3,4-ethylenedioxythiophene)

A noteworthy example of conducting polymer thermoelectric is Poly(3,4-ethylenedioxythiophene) (PEDOT) which is a derivative of polythiophene, emerges as a prominent conducting polymer for thermoelectric applications. PEDOT have specific qualities such as customizable high electrical conductivity upon doping with appropriate dopant, a low-density structure, robust environmental stability, and easy preparation [24-25]. Nevertheless, a key challenge hindering the broader use of PEDOT is its insolubility in water and conventional solvents. This limitation can be effectively tackled by creating an emulsion with polystyrenesulfonic acid (PSS), eventually leading to the formation of an aqueous solution known as PEDOT:PSS.

Remarkably, this aqueous PEDOT:PSS solution has been industrially produced on a large scale due to its common use [26].

Doping and de-doping processes yield significant influence over carrier mobility, carrier density, and oxidation level within conducting polymers, consequently exerting a notable impact on their electrical conductivity and hence Seebeck coefficient [27-29]. The utilization of various chemical agents as dopants further adds this effect, doping substances like dimethyl sulfoxide (DMSO) [30], tetrahydrofuran (THF) [31], and KOH [32]. The secondary doping can be carried out by various methods, including organic polar solvents like ethylene glycol (EG) [33], N,N-dimethylformamide (DMF) [15], N-methyl-2-pyrrolidone [34]. Cosolvents comprising two or more kinds of organic polar solvents alone or with water [35], mixtures of organic solutions and inorganic salts like zinc chloride, copper (II) chloride [39], methylammonium iodide [36-38], various acids such as H_2SO_4 [40] etc. Following the introduction of appropriate dopants, the electrical conductivity of conducting polymers can occasionally undergo a remarkable surge upto multiple orders of magnitude. This augmentation is primarily attributed to the capability of dopants to realign the molecular chains of these polymers, thereby offering improved carrier transport [41].

For instance, Chu et al. observed that the doping of EG, polyethylene glycol, formic acid, and methanol increased the electrical conductivity of pristine films of PEDOT from 0.3 S/cm to 640, 800, 1900, and 1300 S/cm, respectively [42]. Simultaneously, the Seebeck coefficient reduced from 32.3 $\mu V/K$ to almost 20 $\mu V/K$. The achieved zT is of 0.32 at room temperature from PEDOT:PSS films treated with formic acid. The authors attributed the significant enhancement of this film to secondary doping, which increased electrical conductivity by improving carrier mobility and causing alterations in morphological features. Notably, the carrier concentration this material remained constant. The optical images of as prepared flexible film is illustrated in **Figure (6a)**. In contrast, in case of PEDOT-ToS-PPP films (PPP: Polyethylene glycol-Polypropylene glycol-Polyethylene glycol, ToS: tosylate), the treatment using a mixture of $NaBH_4$ and DMSO resulted in enhanced TE efficiency. This enhancement was mainly due to the alteration of the oxidation level of PEDOT, selective removal of

PPP/ToS components, and improved ordering of the PEDOT chains [43]. Furthermore, treating PEDOT:PSS with concentrated H_2SO_4 led to the restructuring of films into highly crystalline nanofibrils as demonstrated in **Figure (6b)**. These films exhibited an electrical conductivity of 4380 S/cm. The surge in conductivity is attributed to charge separated transition mechanism from amorphous PEDOT:PSS to crystalline form via concentrated H_2SO_4 treatment as illustrated in **Figure (6c)** [44]. In this context, the doping of PEDOT with ClO_4^- , PF_6^- and bis(trifluoromethylsulfonyl)imide (BTFMSI) results enhancement of electrical conductivity. However, it was noted that the Seebeck coefficient remained largely unaffected [45]. Luo et al. reported adding of DMSO to a PEDOT:PSS solution, followed by spin casting. Subsequently, a post-treatment was carried out on the thin PEDOT:PSS film using a mixture of DMSO and the ionic liquid 1-ethyl-3-methylimidazolium tetrafluoroborate (EMIM- BF_4). The addition of DMSO to PEDOT:PSS resulted in the formation of an interconnected network with elongated PEDOT grains. This configuration led to a maximum power factor (PF) of $30.1 \mu\text{W m}^{-1} \text{K}^{-2}$, with an electrical conductivity (σ) of 930.41 S cm^{-1} and a Seebeck coefficient (α) of $17.99 \mu\text{VK}^{-1}$. Additionally, the post-treatment involving EMIM- BF_4 induced an interconnected network of shorter and circular PEDOT grains, leading to an increase in polaron density. This enhancement in polaron density further improved the Seebeck coefficient and maximized the power factor (PF) to $38.46 \mu\text{W m}^{-1} \text{K}^{-2}$ [46]. Similarly another group employed a technique in which they mixed PEDOT:PSS with a combination of ethylene glycol (EG) and DMSO, followed by immersion in an EG solution [47-48]. This method successfully reduced the thickness of the PSS layer, which in turn enhances the mobility of charge carriers due to the decreased tunneling distance between conductive domains. This approach resulted in simultaneous improvements in both electrical conductivity (σ) and Seebeck coefficient (α). Furthermore, the thermal conductivity was lowered from 0.30 to $0.22 \text{ W m}^{-1} \text{K}^{-1}$ for DMSO-mixed PEDOT:PSS and from 0.32 to $0.23 \text{ W m}^{-1} \text{K}^{-1}$ for EG-mixed PEDOT:PSS.

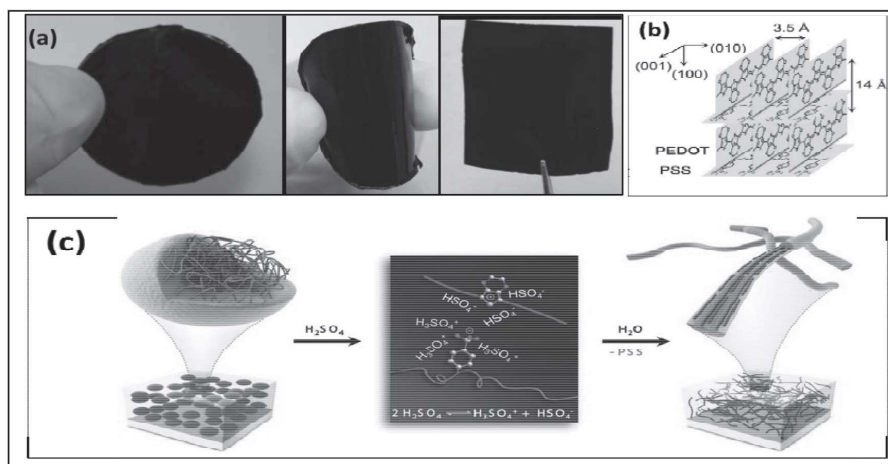


Figure 6: (a) Photographs of flexible PEDOT:PSS bulky papers in different shapes, (Reprinted from Ref. [42] with permission from American Chemical Society) (b) Molecular packing structure of crystalline PEDOT:PSS, (c) Diagram of the structural rearrangement of PEDOT:PSS. The amorphous PEDOT:PSS grains (left) are reformed into crystalline PEDOT:PSS nanofibrils (right) via a charge-separated transition mechanism (middle) via a concentrated H_2SO_4 treatment. (Reprinted from Ref. [44] with permission from John Wiley and Sons).

Also, de-doping has emerged as a significant technique to enhance the Seebeck coefficient of PEDOT:PSS by reducing the carrier concentration. This strategy involves various approaches, including the manipulation of the gate voltage in the organic electrochemical transistor configuration [49], utilization of chemical reducing agents such as hydrazine [50-51], sodium sulfite (Na_2SO_3) [52], tetrakis(dimethylamino)ethylene (TDAE) [52], sodium borohydride (NaBH_4) [52], hydroiodic acid (HI) [53], and 1-ethyl-3-methylimidazolium tetrafluoroborate (EMIM- BF_4) [54], as well as adjustments to their acidity [55].

Similarly, the addition of substances like sorbitol and TDAE has demonstrated positive outcomes in enhancing the power factor of PEDOT:PSS, resulting in values of $7.26 \mu\text{W}/\text{mK}^2$ and $22.28 \mu\text{W}/\text{mK}^2$, respectively. Notably, the figure of merit of the latter case reached 0.026 at a temperature of 300 K [56]. However, it's important to acknowledge that the inherent toxicity of some organic solvents used in the dedoping process poses a significant limitation. To address this challenge, solvents which are characterized by being cost-effective, easy to prepare and store, biodegradable, biocompatible,

and non-toxic are used. An example of this approach involves the combination of choline chloride and ethylene glycol (EG) as a solvent for PEDOT:PSS, leading to a power factor of $24.08 \mu\text{W}/\text{mK}^2$ [57]. The power factor of PEDOT:PSS films as the function of doping concentration and reaction temperature respectively is shown in **Figure (7a,b)**. Additionally, a fabrication method was devised involving the dispersion of PEDOT:PSS in water followed by the addition of 5% dimethyl sulfoxide (DMSO), and subsequent post-treatment with an optimized concentration of DMSO and hydrazine mixture. The series of reactions resulted a film with a Seebeck coefficient of $142 \mu\text{V}/\text{K}$, electrical conductivity of $2 \text{ S}/\text{cm}$, and power factor of $112 \mu\text{W}/\text{mK}^2$ [51]. The initial sequential treatment was later modified by introducing p-toluenesulfonic acid monohydrate (TSA) into the PEDOT:PSS solution for the purpose of secondary doping. The inclusion of TSA brought changes in both the doping level and the conformation of the polymer chains [58]. Subsequently, a secondary sequential treatment involving DMSO and hydrazine was conducted on the PEDOT:PSS film that had previously undergone treatment with a DMSO/TSA solution with the structural chain deformation to remove PSS. Through these series of experiments an electrical conductivity of $783 \text{ S}/\text{cm}$, a Seebeck coefficient of $50.4 \mu\text{V}/\text{K}$, and a power factor of $318.4 \mu\text{W}/\text{mK}^2$ was achieved [58].

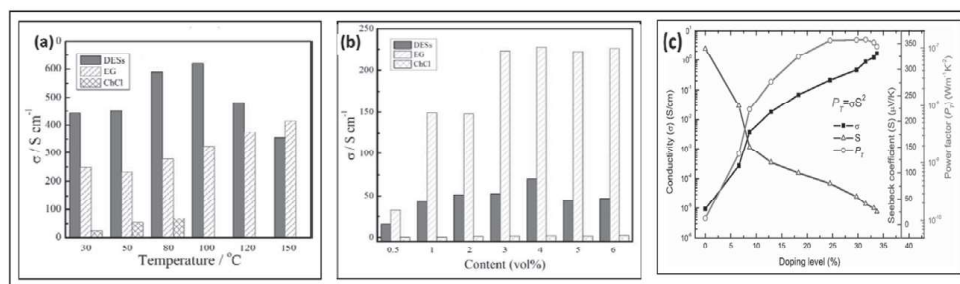


Figure 7: (a) Seebeck coefficient of PEDOT:PSS films containing different amount of various additives, (b) Seebeck coefficient post-treated PEDOT:PSS films using various reagents at different treating temperature, (Reprinted from Ref. [57] with permission from John Wiley and Sons) (c) Doping dependence of the room temperature Seebeck coefficient S (open triangles), electrical conductivity (filled squares), and thermoelectric power factor P (open circles), (Reprinted from Ref. [92] with permission from American Physical Society).

Further, Kim et al. introduced a post-treatment method involving a coating made from a mixture of DMSO and hydrazine (as a reducing

agent) onto a PEDOT:PSS film. This treatment aimed to convert bipolarons into polarons or neutral states within the PEDOT chains. By carefully controlling the concentration of hydrazine (0.0175 wt%), the highest power factor (PF) of $318.4 \mu\text{W}/\text{mK}^2$ was achieved, with an electrical conductivity (σ) of 578 S cm^{-1} and a Seebeck coefficient (α) of $67 \mu\text{V K}^{-1}$ [59]. Also this author demonstrated that the electrical conductivity of PEDOT:PSS can be significantly enhanced through a post-treatment involving H_2SO_4 . This treatment led to an impressive electrical conductivity of 4380 S/cm . The increase in electrical conductivity is correlated with the structural rearrangement of PEDOT:PSS induced by acid. Subsequently, when the PEDOT:PSS film was treated with H_2SO_4 vapor, showed power factor of $17 \mu\text{W m}^{-1} \text{ K}^{-2}$. This value is substantially higher than that of the pristine PEDOT:PSS film, which exhibited a power factor of $0.006 \mu\text{Wm}^{-1}\text{K}^{-2}$ [59]. The improvement in power factor was achieved due to the enhanced Seebeck coefficient and electrical conductivity resulting from the reduction of Coulomb interaction between PSS and PEDOT, as well as the structural rearrangement of the PEDOT:PSS film. Furthermore, Ouyang and co-workers reported when the PEDOT:PSS film underwent a sequence of treatments, including being treated with H_2SO_4 three times and subsequently treated with NaOH, the highest power factor achieved was $334 \mu\text{Wm}^{-1}\text{K}^{-2}$ [60]. In 2018 the same author also reported on a series of post-treatments using various ionic liquids on the surface of PEDOT:PSS. The ionic liquids utilized include 1-ethyl-3-methylimidazolium dicyanamide (EMIM-DCA), EMIM- BF_4 , and 1-ethyl-3-methylimidazolium bis(trifluoromethylsulfonyl)imide (EMIM-TFSI) [61]. Through these post-treatments, they were able to induce the accumulation of cations on the cold side of the material, which in turn enhanced the mean hole energy. This modification resulted in an increase in the Seebeck coefficient (α), a key thermoelectric property. By using EMIM-DCA, these authors achieved exceptional results, reaching a maximum power factor (PF) of $754 \mu\text{Wm}^{-1}\text{K}^{-2}$, along with a high figure of merit value of 0.75. This successful outcome can be attributed to the manipulation of charge carriers through the accumulation of cations, which improved the overall thermoelectric performance of the PEDOT:PSS material. Another approach involved the treatment of the PEDOT:PSS film with a N,N-dimethylformamide (DMF) solution

of ZnCl_2 . This treatment resulted in an impressive combination of properties, including an electrical conductivity of 1400 S/cm, a Seebeck coefficient of $26.1\mu\text{V/K}$, and a power factor of $98.2\mu\text{Wm}^{-1}\text{K}^{-2}$ [62]. Gong et al. conducted a post-treatment method utilizing a combination of DMSO and poly(ethylene oxide) (PEO), resulting in a simultaneous increase in both the electrical conductivity (σ) and the Seebeck coefficient (α). The introduction of PEO, which has a strong interaction with PEDOT, led to the enhancement of bipolarons in the PEDOT backbone. In their measurements, a maximum electrical conductivity of 1061 S/cm and a maximum Seebeck coefficient of $38.4\mu\text{V/K}$ were achieved. This resulted in the highest obtained power factor (PF) of $157.4\mu\text{W/mK}^2$. The best results were observed when PEDOT:PSS was doped with 5% DMSO and 0.3% PEO [63].

Furthermore, to optimize the thermoelectric properties of PEDOT:PSS films, various post-treatment methods have been explored, including the use of different counter ions to replace PSS. These counter ions include perchlorate (ClO_4^-), hexafluorophosphate (PF_6^-), bis(trifluoromethylsulfonyl)imide (TFSI), and tosylate (ToS). These substitutions aim to modify the doping level and alter the structure of the polymer chains, ultimately influencing the electrical and thermal transport properties of the material. In this regard Crispin et al. conducted an experiment where they introduced PEDOT:ToS into the vapor state along with the reducing agent tetrakis(dimethylamino) ethylene (TDAE) for varying periods of time to manipulate the oxidation level of the material [64]. Through this method, authors were able to achieve a range of oxidation levels between 9% and 36%. At the optimal oxidation level of 22%, a maximum power factor (PF) of $324\mu\text{Wm}^{-1}\text{K}^{-2}$ was achieved, resulting in a thermoelectric figure of merit of 0.25 at room temperature. Kim et al. introduced PPPEDOT:ToS, where (PP-PEDOT) was prepared from a combination of pyridine and a triblock copolymer known as poly(ethylene glycol)-poly(propylene glycol)-poly(ethylene glycol) (PEG-PPG-PEG). This material was used as electrodes, and its oxidation level could be adjusted by applying an electrical potential. The optimized films derived from this approach exhibited an electrical conductivity (σ) of 117 S cm^{-1} and a Seebeck coefficient (α) of $930\mu\text{V K}^{-1}$. This led to a good power factor of $1270\mu\text{W m}^{-1}\text{K}^{-2}$, accompanied by a high zT value of 1.02 [65].

4.1.2. Polyaniline

Polyaniline is one of the most studied conducting polymer due to its exceptional thermoelectric properties. To further enhance in the performance various abundant dopants, such as boric acid [66], 5-sulfosalicylic acid (SSA) [67-69], polystyrenesulfonic acid (PSS) [70], methane sulfonic acid [71], HCl [72-77], and notably camphorsulfonic acid (CSA) dissolved in m-cresol as a solvent, have been harnessed to engineer diverse PANI-based thermoelectric (TE) materials due to their ability to amplify the doping process.

Manipulation of the doping level has demonstrated profound effects on PANI chain conformation and conductivity (σ). It should be noted that as carrier density rises, Seebeck coefficient tends to decrease with increasing doping level. Hence, the optimal combination of maximum conductivity (σ) and TE performance in PANI is generally achieved at a protonation degree of 50% (mole ratio of PANI:CSA = 2:1), a ratio widely employed in the fabrication of PANI-based materials [78]. Secondary doping engineering has attained significant interest for the fabrication of PANI composites. In this context Cao et al. demonstrated the efficacy of functionalized protonic acids, notably camphorsulfonic acid (CSA), in protonating PANI emeraldine base, yielding doped PANI solutions in weakly or nonpolar organic solvents. This process induces a substantial enhancement in conductivity (σ) within the range of 100–400 S cm⁻¹ [79-81]. Further Diarmid et al., who explored the influence of CSA doping in various solutions of m-cresol and chloroform on PANI's viscosity, electronic spectra, and conductivity (σ). As the proportion of m-cresol in the solution increased, the conductivity (σ) approached 200 S cm⁻¹ [82-84]. Yao and co-workers unveiled insights into this phenomenon, showing that increasing m-cresol proportion led to surged carrier mobility and reduced hopping barriers, accompanied by expanded PANI-ordered regions. Consequently, a significant increase in conductivity (σ) was observed, ranging from 4.7 to 220 S cm⁻¹, as m-cresol content increased from 0% to 100%. This increment was accompanied by a slight rise in the Seebeck coefficient (S). Notably, an exceptionally high-power factor (PF) of 11 $\mu\text{Wm}^{-1}\text{K}^{-2}$ was achieved, marking a 60-fold increase as compared to chloroform-based systems [84-85]. Profoundly, the incorporation of camphor sulfonic acid (CSA) as a dopant into

PANI has yielded remarkable outcomes. At a temperature of 17 K, this doping process led to the emergence of a Seebeck coefficient measuring 0.58 V/K and an impressive thermoelectric figure of merit (zT) reaching 2.14. These important results were attributed to the phenomenon of phonon drag effect [86]. Similarly it is reported that CSA doped PANI have showcased Seebeck coefficient of $173 \mu\text{V K}^{-1}$ with electrical conductivity of 14 Sm^{-1} which attributed the PF of $3.5 \mu\text{Wm}^{-1}\text{K}^{-2}$ [87].

4.1.3. Polycarbazole

Polycarbazoles (PCz) have witnessed increased utilization in optical, electronic, and sensory devices, driven by their electroactive and photo-physical properties, ease of synthesis, and solubility. Additionally, PCz exhibits favorable thermoelectric (TE) characteristics owing to its well-structured molecular arrangement [88]. Notably, the oxidation of nitrogen atoms within poly(2,7-carbazole) derivatives leads to localized charge accumulation within the structure. This phenomenon results in enhanced Seebeck voltages alongside decreased electrical conductivity [88]. Furthermore, the incorporation of vinylene units into the construction of poly(2,7-carbazolylenevinylene) derivatives offers improved solubility, increased electrical conductivity, while maintaining a consistent Seebeck coefficient. This strategic adjustment can lead to power factor of $4.1 \times 10^{-8} \mu\text{W/mK}^2$ [89]. Additionally, the substitution of alkyl or benzoyl side chains with the carbazole ring and the backbone unit's nitrogen atom enabled the synthesis of PCz derivatives with a remarkable power factor of $10^{-1} \mu\text{W/mK}^2$ [90]. Subsequent exploration display the introduction of FeCl_3 -doped benzothiadiazole-containing molecules. These molecules exhibited electrical conductivity, Seebeck coefficient, and a power factor of 500 S/cm, 70 $\mu\text{V/K}$, and 19 $\mu\text{W/mK}^2$, respectively [91]. These outcomes rank among the most impressive reported TE properties for polymers based on polycarbazole and its derivatives. Overall, it becomes evident that the TE properties of polycarbazole and its derivatives are significantly influenced by the introduction of functional side chains as substitutional constituents.

4.1.4. Poly(3-hexylthiophene)

Poly(3-hexylthiophene) (P3HT) has gained significant popularity as a semiconducting polymer owing to its accessibility, facile

solution processability, and good electrical properties. Remarkable advancements have been made in the realm of thermoelectric (TE) performance using P3HT. Through the introduction of 20–31% acetonitrile doping, the TE power factor of drop-casted P3HT films shows a remarkable increase by three-order of magnitude, with power factor of $0.14 \mu\text{W}/\text{mK}^2$ which is shown in **Figure (7c)** [92]. Subsequent efforts saw the surge of P3HT's power factor to an even higher value of $20 \mu\text{W}/\text{mK}^2$ through the introduction of doping with ferric salt of tri-flimide (TFSI⁻) anions. Moreover, a notable figure of merit (zT) of 0.04 at 340 K was achieved, marking this as the highest zT value reported for P3HT films [93]. These successes underscore the validity of employing solution-based processes for the fabrication of flexible TE devices. Furthermore, P3HT films exhibiting high anisotropy were crafted through polymer epitaxy under a temperature gradient crystallization process, using a 1,3,5-trichlorobenzene template [94]. The schematic representation of ordered film preparation is shown in **Figure (8)**. Near room temperature these films demonstrated maximum values of electrical conductivity, Seebeck coefficient and power factor, reaching 320 S/cm, 269 $\mu\text{V}/\text{K}$ and $62.4 \mu\text{W}/\text{mK}^2$ respectively.

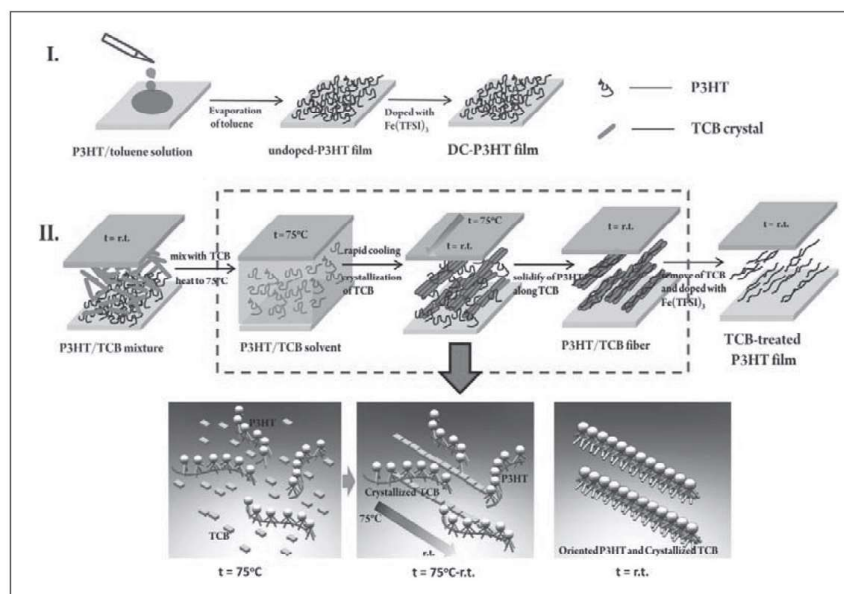


Figure 8: The schematic diagram of preparation of ordered P3HT with fiber-like texture by a two-step process. (I) The comparison P3HT film is prepared by drop-casting and doped by Fe (TFSI)₃ of nitromethane solution (DC-P3HT). (II) The undoped P3HT film is covered by small

molecule 1,3,5-trichlorobenzene (TCB) powder, heated to 75 °C and then cooled rapidly from one side to the other to room temperature, forming a large temperature gradient and TCB solidified as a needle-like crystal along the temperature gradient. The P3HT polymer chains solidify on the TCB surface with polymer chains locking into the lattice of TCB due to the strong π - π conjugated interactions between the thiophene and benzene rings. (Reprinted from Ref. [94] with permission from Springer Nature)

4.1.5. Polyacetylene

Polyacetylene (PA) is formed through the polymerization of acetylene, resulting in a chain featuring recurring alkene groups. PAs exhibit a range of characteristics, including insulating, semiconducting, and metallic behaviors, due to their compatibility with various dopants such as F, I, Cl, and Br. For instance, exceptional electrical conductivities have been achieved, reaching as high as 20,000 S/cm at 300 K [95] and 28,500 S/cm at 300 K [96] in I- and FeCl₃-doped PA films, respectively. It has also been noted that the stretching of I-doped PA films can lead to an enhancement in their electrical conductivity [97]. However, despite their achievements as the first polymers to exhibit high electrical conductivity and power factor, PAs have yet to find extensive application in the realm of thermoelectricity due to their susceptibility to air-induced instability and limited solubility. The tabulated summary of modifications for enhanced thermoelectric properties of conducting polymers is presented in **Table 2**.

Table 2: Tabulated summary for thermoelectric performances of modified organic polymers.

SL. NO.	HOST MATRIX	DOPANT/ DEDOPANT	S μ V/K	σ S/cm	K W/mK	PF μ W/mK ²	ZT	REFER- ENCE
1	PEDOT:PSS	DMSO	33.4 \pm 2.2		0.42 \pm 0.07		0.42	[27]
2	PEDOT:PSS	EG	27.3 \pm 1.9		0.52 \pm 0.11		0.28	[27]
3	PEDOT:PSS	DMSO	12.51	36.17		0.57 L		[30]
4	PEDOT:PSS	KOH	90	0.02				[32]
5	PEDOT:PSS	FORMIC ACID	20.6	1900		80.6	0.32	[42]
6	PEDOT-TOS-PPP	NABH ₄ /DMSO	143.5	5.7	0.451	98.1	0.064	[43]
7	PEDOT	BTFMSI			0.19	147	0.22	[45]
8	DMSO TREATED PEDOT:PSS	EMIM-BF ₄			0.17	38.46	0.068	[46]

SL. NO.	HOST MATRIX	DOPANT/ DEDOPANT	S $\mu\text{V/K}$	$\bar{\sigma}$ S/cm	K W/mK	PF $\mu\text{W/mK}^2$	ZT	REFER- ENCE
9	PEDOT:PSS	SORBITOL/ TDAE			0.013-0.039	22.28	0.026	[56]
10	PEDOT:PSS	CHOLINE CHLORIDE AND EG	29.1	620.6	0.17	24.08	0.042	[57]
11	DMSO/TSA TRATED PEDOT:PSS	DMSO AND HYDRAZINE HYDRATE	50.4	783		318.4		[58]
12	PEDOT:PSS	DMSO/ HYDRAZINE	67	578		318.4		[59]
13	PEDOT:PSS	H ₂ SO ₄	37.1 \pm 2.9	2170 \pm 201		334 .0		[60]
14	PEDOT:PSS	EMIM-DCA				754	0.75	[61]
15	PEDOT:PSS		23.3	596		32.5		[125]
16	PPPEDOT: TOS		930	117		1270		[65]
17	PANI	M-CRESOL	20	220		11		[85]
18	PANI	CSA	173	14		3.5		[87]
19	PCZ	FECL ₃	70	500		19		[91]
20	PCZ	VENYL	600	5.3 X 10 ⁻³		4.1 $\times 10^2$		[89]
21	P3HT	NOPF/ ACETO NITRILE	25	1		0.14		[92]
22	P3HT	FERRIC SALT	65	92	0.2	20	0.04	[93]
23	P3HT	1,3,5 - TRICHLORO- BENZENE	320	269		62.4	0.1	[94]
24	POLYACE TYLENE (PA)	IODINE	17	10000				[97]

4.2. Inorganic- Polymer Nanocomposite Thermoelectrics

In recent years, there have been significant advancement in improving the thermoelectric properties of conducting polymers. However, the enhancements of zT values, particularly for n-type conducting polymers, remain relatively constrained. To achieve higher zT values, researchers have turned to the development of hybrids that combine polymers with inorganic materials. These hybrids benefit the inherent low thermal conductivity and flexibility of polymers, while also benefiting from the superior Seebeck coefficient (S) provided by inorganic materials. In the context of inorganic-polymer thermoelectric composites, the inorganic materials serve as fillers, while the polymers function as the host matrices. This arrangement

allows for combination of the unique properties of each component, ultimately leading to improved thermoelectric performance.

In inorganic-conducting polymer composites, tellurium-based inorganic materials are highly regarded for their exceptional thermoelectric performance at room temperature. These materials are considered among the best options for room-temperature thermoelectric applications. As a result, they have found widespread use in such composites, contributing to their enhanced thermoelectric properties. For instance, Yong et al. reported the power factor of $2.54 \mu\text{Wm}^{-1}\text{K}^{-2}$ with the electrical conductivity of 8.1 S/cm for Bi_2Te_3 /polythiophene (PTH) composite which was sintered at 623K at 80 MPa . This composite produced relatively higher power factor values to the other samples which were sintered at different temperatures [98]. Similarly, the hybrid PEDOT:PSS/ Bi_2Te_3 -NWs film were successfully prepared by two different methods such as spin coating and drop casting and the process of preparation is shown in **Figure (9)** [99]. The prepared composite film containing 10 wt% Bi_2Te_3 -NWs exhibited significantly higher electrical conductivity (401 Scm^{-1}) and power factor ($10.6 \mu\text{Wm}^{-1}\text{K}^{-2}$) compared to the layer-by-layer assembly film. Notably, the Seebeck coefficient remained constant in hybrid films despite an increase in the Bi_2Te_3 -NWs content, which differs from the behavior observed in layered films. Furthermore, the PEDOT:PSS/ Bi_2Te_3 -NWs pellets demonstrated a larger Seebeck coefficient ($54 \mu\text{VK}^{-1}$) but a lower electrical conductivity (12.4 Scm^{-1}), resulting in a lower power factor. Next, Bi_2Te_3 -based alloy nanosheets (NSs) and PEDOT:PSS composite film was successfully prepared using both spin coating and drop casting techniques. As the content of Bi_2Te_3 -based alloy nanosheets (NSs) increased from 0 to 4.10 wt%, the composite film exhibited concurrent improvements in electrical conductivity and Seebeck coefficient. Specifically, the drop-cast composite film containing 4.10 wt% Bi_2Te_3 -based alloy nanostructures achieved a good electrical conductivity of 1295.21 S/cm . This value surpassed both the electrical conductivity of a dimethyl sulfoxide-doped PEDOT:PSS film (753.8 S/cm) prepared under the same conditions and the range of electrical conductivity observed in Bi_2Te_3 -based alloy bulk materials. Moreover, the composite film demonstrated a high-power factor, reaching approximately $32.26 \mu\text{Wm}^{-1} \text{ K}^{-2}$ [100].

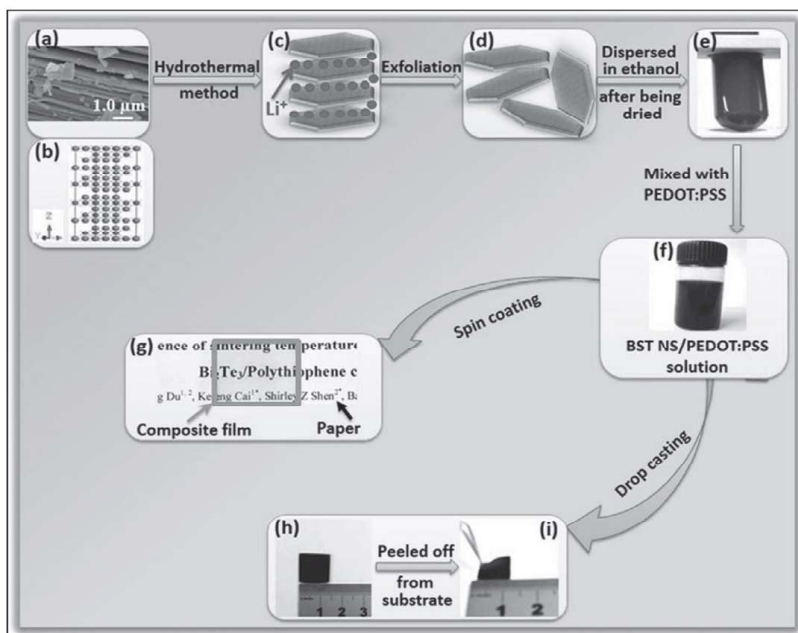


Figure 9: Schematic illustration of the process for preparation of BST NS/PEDOT:PSS films, (Reprinted from Ref. [99] with permission from American Chemical Society)

Another group produced thermoelectric nanocomposite films using PEDOT:PSS, PVA, and Bi_{0.5}Sb_{1.5}Te₃ nanocrystals [101]. These films demonstrate a better characteristic. At 300 K, they exhibit a power factor of 47.7 μWm⁻¹K⁻² and a zT value of 0.05, indicating efficient heat-to-electricity conversion. These films are mechanically robust, boasting a tensile strength of 79.3 MPa. Despite their strength, they remain highly flexible, with a fracture strain of 32.4%. These attributes make them ideal for applications in textile manufacturing, meeting both thermoelectric and mechanical requirements. Even though the promising results of composites consist of tellurium alloys, Te composites are also explored by scientific community [102-104,130]. For example, See et al. created nanocomposites consisting of Te nanorods and PEDOT:PSS during solution casting and is presented in **Figure (10a)** [102]. The excellent uniformity of composite film on quartz substrate is picturized and is displayed in **Figure (10b)**. These composites provide the combined benefits of these materials. Te nanorods exhibit a high Seebeck coefficient of 408 μV/K at room temperature. PEDOT:PSS possesses a low thermal conductivity ranging from 0.24 to 0.29 μWm⁻¹K⁻¹ at room temperature. The

synergistic effect of combining Te nanorods with high Seebeck coefficient and PEDOT:PSS with low thermal conductivity led to the achievement of a remarkable power factor of $70.9 \mu\text{W m}^{-1}\text{K}^{-2}$ and zT value of 0.1 at room temperature. Song and group reported that, in the PEDOT/PSS/Te (90 wt.%) composite films, the Seebeck coefficient is approximately $191 \mu\text{V/K}$, a substantial improvement compared to pristine PEDOT/PSS [103]. To further enhance the thermoelectric properties of these composite films, H_2SO_4 treatment was employed. The electrical conductivity of the composite films significantly increased from 0.22 S/cm to 1613 S/cm . This enhancement occurred due to the removal of insulating PSS and structural rearrangement of the PEDOT component. An optimized power factor of $42.1 \mu\text{W/mK}^2$ was achieved at room temperature for a PEDOT/PSS/Te (80 wt.%) sample. This value is approximately ten times greater than that of the untreated PEDOT/PSS/Te composite film. Furthermore, layered hybrid materials can be prepared using certain inorganic materials which intrinsically possess layered structures. Examples of such layered inorganic materials include Bi_2Te_3 , SnSe , TaS_2 , MoS_2 , Na_xCoO_2 , and TiS_2 [105-107]. As an example Wan et al. reported that for the hybrid superlattice composed of $\text{TiS}_2/[(\text{hexylammonium})_x(\text{H}_2\text{O})_y(\text{DMSO})_z]$, Electrical conductivity of 790 S/cm and power factor $0.45 \text{ mW m}^{-1}\text{K}^{-2}$ was obtained [107]. Furthermore, this material exhibited an in-plane lattice thermal conductivity of $0.12 \pm 0.03 \text{ W m}^{-1}\text{K}^{-1}$. Remarkably, this thermal conductivity is two orders of magnitude smaller than single-layer and bulk TiS_2 . The combination of a high-power factor and low thermal conductivity contributed to the attainment of a thermoelectric figure of merit which reached a value of 0.28 at 373K. Apart from these the inorganic-non-conducting polymer composites gaining significant interest in the TE field owing to their improved thermoelectric properties. For instance, Jiang et al. reported the ultra high-power factor for Polyvinyl pyrrolidone- Ag_2Se composite deposited on nylon membrane [108]. Due to the unique microstructure and synergistic effects, an optimal composite film showcases an exceptionally high-power factor, approximately $1910 \mu\text{Wm}^{-1}\text{K}^{-2}$, which corresponds to a zT value of approximately 1.1 at 300 K. Author also compared these values with some reported power factor values of TEGs. As the evident example of transition metal and its compound composite it is noteworthy to mention that Chen et

al. observed an abnormal decoupling phenomenon in Ni nanowire-PVDF composites as the Ni nanowire content increased [109]. In these composites, the electrical conductivity and power factor reached approximately 4700 S/cm and 200 $\mu\text{Wm}^{-1}\text{K}^{-2}$ at room temperature when the composites contained 80 wt% Ni nanowires. Furthermore, they achieved a maximum zT value of 0.15 at 380 K. Alongside their excellent flexibility is optically imaged and these measurements are shown in **Figure (10c)**. Similarly, the fabricated freestanding flexible composite thin films consisting of $\text{Cu}_{1.75}\text{Te}$ nanowires and PVDF films exhibits an electrical conductivity of 2490 S/cm, a Seebeck coefficient of 9.6 $\mu\text{V/K}$, and a power factor of 23 $\mu\text{W m}^{-1} \text{K}^{-2}$ at room temperature [110]. The summarized tabulations of such nano composites for thermoelectric performances are presented in **Table 3**.

Table 3: Summary of polymer-inorganic nanocomposites for thermoelectric applications

Sl. No.	Host Matrix	Inorganic Filler	S $\mu\text{V/K}$	σ S/cm	K W/mK	PF $\mu\text{W/mK}^2$	zT	Reference
1.	Polythiophene (P3HT)	Bi_2Te_3	-55	8.1		2.54		[98]
2.	PEDOT: PSS	Bi_2Te_3 -NWs	16.3	401		10.6		[99]
3.	PEDOT: PSS	Bi_2Te_3		1295.21		32.26		[100]
4.	PEDOT: PSS/ PVA	$\text{Bi}_{0.5}\text{Sb}_{1.5}\text{Te}_3$	144	23		47.7	0.05	[101]
5.	PEDOT: PSS	Te	408		0.24	70.9	0.1	[102]
6.	PEDOT: PSS	Cu_2Se	78.2	470		287.4		[128]
7.	PEDOT: PSS (treated with H_2SO_4)	Te	191	1613		42.1		[103]
8.	[(Hexylam-monium) $_x(\text{H}_2\text{O})_y(\text{DMSO})_z$]	TiS_2	-78	790	0.12 ± 0.03	450	0.28	[107]
9.	PVP	Ag_2Se	-143.4			1910	1.1	[108]
10.	PVDF	Ni-NWs		4700		200	0.15	[109]
11.	PVDF	$\text{Cu}_{1.75}\text{Te}$	9.6	2490		23		[110]
12.	PEDOT:PSS/PVA	Te	11.3	382.4		8.5		[126]
13.	PEDOT	Te	290	28		235		[128]
14.	PEDOT:PSS	SnS	29.38	210.4		38.04		[132]

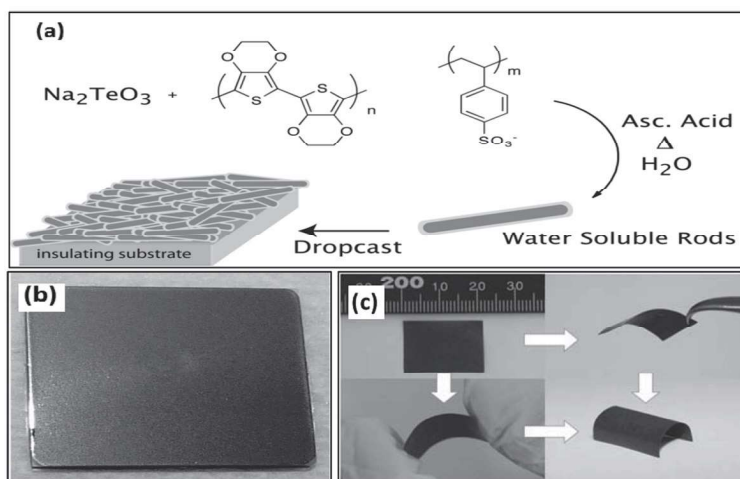


Figure 10: (a) Synthesis of PEDOT:PSS passivated Te nanorods, followed by formation of smooth nanocomposite films during solution casting, (b) picture of a typical drop-cast composite film on a 1 cm^2 quartz substrate, illustrating excellent film uniformity, (Reprinted from Ref. [102] with permission from American Chemical Society) (c) Typical photographs of highly bendable Ni/PVDF TENC film, (Reprinted from Ref. [109] with permission from John Wiley and Sons).

4.3. Carbon Based Flexible Thermoelectrics

Another alternative strategy for the conventional inorganic TE materials involves organic π -conjugated semiconductors. Recently, carbon-based nanostructures such as carbon nanotubes, graphene and many more, offers new opportunities as desirable composite flexible thermoelectric materials, owing to their admirable properties that include lower thermal conductivity value, non-toxicity, earth abundance, lightweight, flexible, and solution processible properties [111]. By functionalizing the large surface area and junctions in carbon nanotubes mat, Suk Lae Kim and team developed both p- and n-type fabric-like flexible lightweight materials from the poor thermo power and only p-type characteristics of typical CNTs [112]. The experimental investigation about changes in energy band diagram interpreted about the carrier type and relatively large thermopower. On other hand, π -conjugated structure and large specific surface area of carbon nanomaterials provide the intimate contact with the conductive polymer, hence enhancement of interfacial effect on the phonon scattering results lower thermal conductivity. Finally, a strong intimate contact between carbon nanostructures and conductive polymer explores the composite with

improved thermoelectric properties. For instance, Muller's research group demonstrated thermoelectric behaviour of the polymer can be improved by interfacing the conduction polymer with carbon nanotubes. These authors also noticed that the improvement not only induced by optimizing the level of polymer doping, but also changing the solution processing process [133]. Therefore, such composites received considerable attention in the research, in which carbon nanostructure are the filler for thermoelectric. Hence, considering all these into account carbon based flexible thermoelectric materials are reviewed.

Carbon nanotubes (CNTs) are the type of tubular graphitic macromolecule considered as promising candidates in nanocomposite materials. They also exhibit better thermoelectric activity with zT around 0.4-0.8 at 1000 K. For instance, doping of spun carbon nanotubes directly with benzyl viologen leads to maximum power factors of $3103 \mu\text{Wm}^{-1}\text{K}^{-2}$, which is almost close to those of Bi_2Te_3 compounds [113]. The flexibility, electrical conductivity, mechanical strength other multifunctional properties of CNTs are essentially required, a great effort have been made to improve the performance of polymer matrix by introducing CNTs as a nanofiller. But still these composites face many challenges like weak intimate contact between carbon nanotubes and polymer matrix, limitations of dispersion and doping. Recently, influence of carbon nanotubes and their mass fraction into polymer matrix on the electrical conductivity was systematically investigated by Wu et al [114]. Author designed a new layer-by-layer deposition approach as schematically illustrated from the **Figure (11)**, the fabrication of CNTs and polyvinyl alcohol composite fibers. The in situ mixing of these two materials at molecular levels, results in uniform dispersion to infiltrate in to efficiently formation of fibers. At the same time, there is an increasing the strength and conductivity from 50 to 1255 MPa and 0 to 2000 Scm^{-1} respectively due to grown of different diameter of CNTs and difference in the incorporation of mass fractions. Similarly, another group demonstrated same factors by preparing CNTs and P3HT composite film using solution mixing method, in which diameter of CNTs was in the range from 8 nm to 50 nm [115]. Importantly, maximum power factors of $49 \mu\text{Wm}^{-1}\text{K}^{-2}$ achieved for the less than 8 nm diameter of CNTs and 5% mole fraction. This superior TE power factors of composite film (CNT <

8 nm) can be attributed to the heterogeneous dispersion of shorter length CNTs as well as fully connected interlayer of polymer, which make delocalization carrier movement over the entire network along the π - π conjugated region. Apart from this, generally, there are two types of carbon nanotubes, namely, single walled carbon nanotubes (SWCNTs) and multi walled carbon nanotubes (MWCNTs). Among these two, SWCNTs shows the semiconducting features determined by their stereochemistry, and these are widely used in electronic devices like field effect transistors, and solar cells.

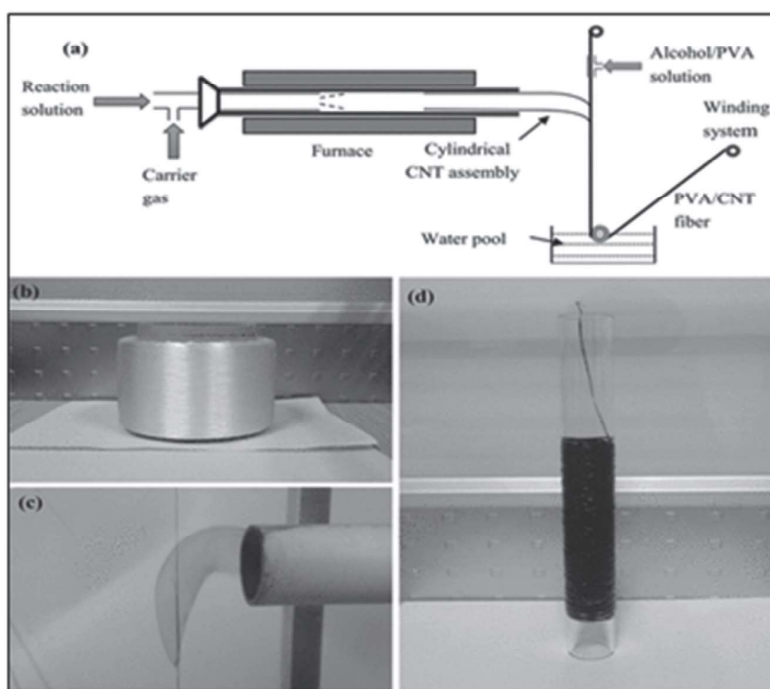


Figure 11: (a) Schematic illustration of the deposition process. A substrate wire is wetted with an alcohol/PVA solution, supplied to the reactor for deposition of CNT assembly, and finally wound up. (b) Vinylon wire used as the substrate for depositing the first layer of CNTs, (c) Hollow cylindrical CNT assembly shrinking and depositing on the substrate wire which is wetted with an alcohol/PVA solution, (d) CNT/PVA composite fiber wound on a glass tube, (Reprinted from Ref. [114] with permission from American Chemical Society)

Moreover, it was found that SWCNTs show relatively better thermoelectric features, and they are inherently flexible, hence potential for the creation of flexible thermoelectric nanocomposites with other materials. Yao's research group prepared SWCNTs and PANI composite films using a simple solution process with controlled

the content of SWCNTs [116]. The improved conductivity and Seebeck coefficient achieved up to 769 Scm^{-1} and $65 \mu\text{VK}^{-1}$ respectively, which is several times larger than those of carbon nanotubes and pure PANI films. Consequently, maximum thermoelectric power factor and zT values reached $176 \mu\text{Wm}^{-1}\text{K}^{-2}$ and 0.12 respectively at room temperature. Similarly, SWCNTs and poly (vinylidene fluoride) composite fiber was prepared through wet spinning method. Here, the author noticed the influence of dispersion rate of SWCNTs on the mechanical strength of the composite fiber. After systematic optimization, the p- and n-type composite fibers of these two components were achieved with power factors 380 and $290 \mu\text{Wm}^{-1}\text{K}^{-2}$ respectively. It is well known that, some of the small organic molecules (OSM) such as porphyrin, bis (ethyleledithio) tetrathiafulvalene (BEDTTTF) and etc., have been studied in last decade in detail as thermoelectric materials [117]. But, these OSM exhibits lower power factor (Maximum in the range from 100 to $200 \mu\text{Wm}^{-1}\text{K}^{-2}$ then organic materials. Therefore, in order to enhance thermoelectric properties, these molecules can be used as filler or coating materials in composite materials. For instance, copper phthalocyanine (CuPc)/ SWCNTs p-type composite was fabricated using high energy ball milling method. Due to synergetic and large interfaces of composite results in strong acceptor- donor, and interaction of π - π conjugation structures lead to high degree ordered face stacking of OSM in composite, which permits further to improve the carrier concentration and carrier mobility. Finally, optimized composite of these two components displayed a maximum power factor of $70.1 \mu\text{Wm}^{-1}\text{K}^{-2}$ [117]. On other hand, there is a literature that establishes that high electrical conductivity and mechanical properties of graphene is potential for thermoelectric materials based on above molecules of organic materials. It is expected that high electrical conductivity of graphene and low thermal conductivity of organic thermoelectric materials combination will afford better performance. Alongside, when the uniform dispersion of graphene in the polymer network takes place, graphene and polymer composite has higher ability to improve the thermoelectric features owing to the availability of large surface area, and stronger π - π interaction of graphene. As per the literature, graphene can enhance the interfacial area as compared to carbon nanotubes, while after addition of 2 to 3% of graphene incorporation into polymer (PEDOT:PSS) matrix

induce the 10 times improved the zT values, and is much greater than carbon nanotube based composite. Recently, fullerenes also gained a significant interest in the field of thermos-electrics and continuous efforts have been putting to enhance the thermoelectric properties of graphene based composites. The introduction of reduced grapheme oxide (rGO) which is non-covalently functionalized by fullerene into PEDOT: PSS network. In this system, fullerene can enhance the relative seeback coefficient and electrical conductivity by graphene with lower thermo-power. Due to strong synergetic effect of these two components, maximum zT reached up to 0.067 and is several times higher than single components filled thermometric materials. From the above reports, it can be concluded that larger surface area, flexibility, greater electrical conductivity, and other multifunctional properties of carbon based nanostructure can be synergetic composites to achieve the excellent thermoelectric performance.

Table 4: Summary of carbon based polymer

Sl. No.	Host Matrix	Carbon Based Fillers	S $\mu\text{V/K}$	σ S/cm	PF $\mu\text{W/mK}^2$	zT	Reference
1.	Polyvinyl Pyrrolidone (fluoride)	Carbon nanotube	----	----	378 ± 56	----	[112]
2.	Carbn nanoparticles	Carbon nanotubes	54.0 ± 1.4	----	503 ± 49	----	[134]
3.	benzyl violegen	Carbon nanotubes	----	2228	3103	----	[135]
4.	Polyvinyl Alcohol	Carbon nanotubes	----	2000	-----	----	[114]
5.	CNT/poly(3-hexylthiophene)	Carbon nanotubes	27.8	36.2	49	----	[115]
6.	PANI	SWCNTs	65	769	176	0.12	[116]
7.	1,3,6,8-tetrakis (3,6-di-tert-butyl-9H-carbazol-9-yl)pyrene	Carbon nanotubes	79.2	46.6	48.0	----	[136]

4.4. Inorganic Thermoelectrics Deposited on Flexible Substrate

The development of thin film thermoelectric materials on flexible substrates represents a promising avenue for advancing flexible and portable energy harvesting devices. This emerging field has gathered significant attention due to its potential applications in wearable

electronics, flexible sensors, and portable power generation. In this context, various deposition techniques have been explored to create thin film thermo-electrics on organic substrates, with objective being the integration of active thermoelectric materials onto flexible and lightweight substrates. Among the methodologies employed for this purpose, magnetron sputtering, co-evaporation, spin-coating, and screen printing have emerged as key techniques. Each of these methods offer distinct advantages and can be tailored to specific material requirements and device designs. Thin film flexible thermoelectric energy conversion devices have been successfully fabricated on a variety of substrates, including Polyimide (PI), Polydimethylsiloxane (PDMS), Polyethylene terephthalate (PET), polyethersulfone (PES), paper and glass fabric [118-124]. These substrates have demonstrated their versatility and compatibility with flexible thermoelectric technology, making them valuable choices for diverse applications in the field of flexible and portable energy harvesting. For instance, Chen et al. presented the development of a highly flexible thermoelectric generator utilizing inkjet-printing technology [118]. Specifically, employing inkjet printing to deposit nanowires (NWs) of Bi_2Te_3 and $\text{Bi}_{0.5}\text{Sb}_{1.5}\text{Te}_3$ on to a polyimide substrate, forming the n-type and p-type legs essential for TEG operation. To enhance the thermoelectric performance of the printed NWs, these authors subject them to a post-print thermal annealing process. It reveals promising results, with a maximum power factor of $180 \mu\text{Wm}^{-1}\text{K}^{-2}$ and $110\mu\text{Wm}^{-1}\text{K}^{-2}$ achieved for the Bi_2Te_3 and $\text{Bi}_{0.5}\text{Sb}_{1.5}\text{Te}_3$ nanowires, respectively. Moreover, when assembled these printed components into a fully functional thermoelectric device, they attain a maximum power output of 127 nW, demonstrating the potential of this flexible thermoelectric generator even at relatively low temperature gradient (32.5 K). Similarly, Ding et al. reported the ink jet printing of Bi_2Te_3 nano pallets with rGO solution on the flexible PI substrate. It was observed that 1% rGO/ Bi_2Te_3 composite films demonstrate remarkable electrical conductivity, with a value of 199.9 S cm^{-1} at 300 K. This high electrical conductivity contributes to the excellent power factor exhibited by these films, which reaches $3.2 \mu\text{Wcm}^{-1}\text{K}^{-2}$ at 300 K and further increases to $4.6 \mu\text{W cm}^{-1} \text{K}^{-2}$ at 400 K [119]. Furthermore, the films containing 1% rGO displayed the highest zT values, reaching 0.2 at 300 K and 0.4 at 400 K. The fabricated

flexible thermoelectric generator using 1% rGO-Bi₂Te₃ composites showed a substantial enhancement in performance. Specifically, at a temperature gradient of 20 K, these TEG devices achieved P_{\max} of 1.72 μW . Further producing P_{\max} of up to 15.22 μW was possible when subjected to a temperature difference of 60 K [119].

On other hand, as the noteworthy example, Mallick et al. reported a high-performance n-type thermoelectric material based on Ag–Se, which are successfully printed onto a flexible PET substrate [120]. This material exhibits Seebeck coefficient of 220 μVK^{-1} and power factor of 420 $\mu\text{W m}^{-1}\text{K}^{-2}$. Moreover, the figure-of-merit (zT) for this printed material reaches 0.6 with thermal conductivity approximately 0.30 $\text{Wm}^{-1}\text{K}^{-1}$. Utilizing this high-performance n-type material, a flexible folded thermoelectric generator was constructed consisting of 13 thermocouples. It generates an open-circuit voltage of 71.1 mV when subjected to a temperature difference (ΔT) of 30 K and a higher voltage of 181.4 mV at a larger ΔT of 110K. Further, another group deposited Ag₂Te nanoparticles (NPs) aqueous solution on the flexible PES substrate which exhibited Seebeck coefficient and electrical conductivity of 1330 μVK^{-1} and 0.037 S/m respectively. Giving rise to the ultimate power factor of 0.66 $\mu\text{Wm}^{-1}\text{K}^{-2}$ [121]. Javash et al. reported the print and sinter solution-processed Bi₂Te_{2.7}Se_{0.3} nanoplate inks onto virtually any flexible substrates such as paper or PI, a transformative 3D conformal aerosol jet printing and rapid photonic sintering process etc. [122]. The electrical conductivity of the printed film undergoes a remarkable transformation within seconds of photonic sintering, transitioning from a nonconductive state to a highly conductive state, measuring at $2.7 \times 10^4 \text{ Sm}^{-1}$ exhibiting an impressive room temperature power factor of 730 $\mu\text{Wm}^{-1}\text{K}^{-2}$. The printed hexylammonium titanium disulfide (TiS₂(HA)_x) nanocomposite on the paper substrate with varied concentration of hexylammonium (HA) displayed the electrical conductivity of $422 \pm 80 \text{ Scm}^{-1}$ for varying concentration of HA from 10 mg to 170 mg for 20 mg of TiS₂. Moreover, Seebeck coefficient of $-101 \pm 20 \mu\text{VK}^{-1}$ is obtained giving rise to power factor of $207 \pm 81 \mu\text{Wm}^{-1}\text{K}^{-2}$ for 80mg HA for 20 mg TiS₂. The as fabricated flexible thermoelectric generator with PEDOT:PSS as counter substrate for (TiS₂(HA)_x) gives P_{\max} of 22.5 nW [123]. Further the fabrication of flexible thermoelectric generator reported by Kim et al [124]. In the fabrication process, a screen-printed material is utilized which

comprises combination of p-type $\text{Bi}_{0.3}\text{Sb}_{1.7}\text{Te}_3$ and n-type $\text{Bi}_2\text{Se}_{0.3}\text{Te}_{2.7}$ thick films. These films are screen-printed onto a quartz substrate. To create a flexible thermoelectric generator, a screen printing technique and a laser multi scanning lift-off process are employed. Specifically, a screen-printed TEG is produced on a $\text{SiO}_2/\text{a-Si}/\text{quartz}$ substrate using both the screen printing technique process and the laser multi scanning process. Using these techniques they constructed prototype f-TEG, which consists of an array of 72 thermoelectric couples. This device exhibits remarkable flexibility at various bending radii while maintaining excellent output performance, delivering $4.78 \text{ mW}/\text{cm}^2$ at a temperature difference (ΔT) of $25 \text{ }^\circ\text{C}$. It was observed that the device's performance remains stable even after undergoing repeated bending for 8000. **Figure 12a and 12b** demonstrate the internal resistance stability under bending stress and durability as the function of bending cycles respectively. **Table 5** summarizes the the thermoelectric performances of inorganic materials deposited on different flexible substrates.

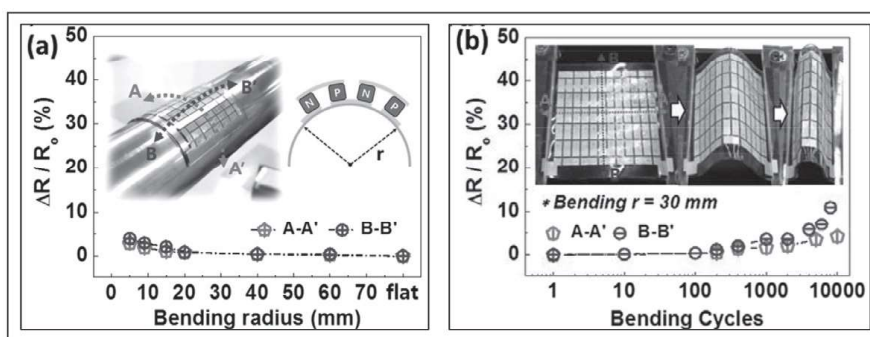


Figure (12):(a) Internal resistance stability under bending stress along both horizontal (A–A') and vertical (B–B') directions, as illustrated in the inset, (b) Durability test through multiple strain cycles with a bending radius of 30 mm. The inset shows photographs of the f-TEG in the flat state and the bending state, (Reprinted from Ref. [124] with permission from American Chemical Society)

Table 5: Summary of thermoelectric performances for inorganic materials deposited of the flexible substrate.

Sl. No.	Host Matrix	Inorganic Deposits	S $\mu\text{V}/\text{K}$	σ S/cm	K W/mK	PF $\mu\text{W}/\text{mK}^2$	zT	Reference
1.	Polyimide	Bi_2Te_3				180		[118]
2.	Polyimide	$\text{Bi}_{0.5}\text{Sb}_{1.5}\text{Te}_3$				110		[118]
3.	Polyimide	RGO/ Bi_2Te_3	-130	199.9		320	0.2	[119]

4.	Polyethylene terephthalate	Ag ₂ Se	220		0.3	420	0.6	[120]
5.	Polyethersulfone	Ag ₂ Te	1330	0.037		0.66		[121]
6.	Polyimide/paper	9e _{2,7} Se _{0,3}		2.7×10 ⁴		730		[122]
7.	Paper	(TiS ₂ (HA) _x)	-101 ± 20	422 ± 80		207 ± 81		[123]
8.	Polyimide	Ag _{1,9} Te	65.2	523.3		222.5		[131]

5. Summary and Outlook

In conclusion this review overlooks the history and key developments in the journey of thermo-electrics and provides the theoretical horizon to thermoelectric parameters such as Seebeck coefficient, electrical conductivity and thermal conductivity and their dependence on carrier concentration. Further it discusses about balancing of these key parameters to enhance power factor and zT values by means of state of art strategies. Moreover, the obstacles in rigid inorganic thermoelectric materials toward the fabrication of flexible and shape engineerable devices are overviewed, which intern projects flexible thermoelectric as the potential candidate for such applications.

Conducting polymers thermoelectric properties depend on their chemical structure and microstructure. These materials derive their thermoelectric properties from π -conjugated bonds, where delocalized π -orbital electrons create molecular π -orbitals. Enhancing their zT value involves methods like doping, de-doping, post-treatment and optimizing crystallinity and alignment. Doping introduces electrons (p-type) or removes electrons (n-type) through oxidation and reduction reactions, enabling control over their electronic characteristics. Further the post treatment techniques enable the polymer structures to arrange in order to enhance the TE performances. However, further optimization of technological conditions and processes is needed to maximize their thermoelectric performance and stability. Moreover, zT of inorganic/polymer composites are quite satisfactory with the synergic effects of high Seebeck coefficient and electrical conductivity of nano thermoelectric fillers with the low thermal conductivity of polymers acting as host. The key pros in these categories include the easy synthetic techniques with tailored morphology of nano fillers with desirable flexibility. But it also face obstacles such as toxicity of well performing inorganic fillers such as Bi-Te compounds and the inhomogeneous distribution of nano fillers etc. Further the need of

non-toxic and light element thermoelectric nanofillers possess this field as prominent candidate for further research.

The exploration of organic π -conjugated semiconductors and carbon-based nanostructures such as carbon nanotubes (CNTs) and graphene have opened up exciting possibilities for alternative flexible thermoelectric materials presenting several key advantages. These materials exhibit lower thermal conductivity, less toxicity, abundant availability, lightweight properties, flexibility and processibility using solution-based methods. Researchers have employed these properties to develop flexible thermoelectric materials with improved performance. In summary, carbon-based nanostructures including CNTs, SWCNTs, MWCNTs and graphene have provided a platform for the development of flexible thermoelectric materials with enhanced properties. These materials offer larger surface areas, flexibility, superior electrical conductivity, and other multifunctional characteristics that enable the creation of high-performance thermoelectric composites with polymers holding significant promise for future thermoelectric applications. Another prominent category in flexible thermoelectric include, thermoelectric thin films deposited on a range of substances such as Polyimide (PI), Polydimethylsiloxane (PDMS), Polyethylene terephthalate (PET), polyethersulfone (PES), paper, and glass fabric by employing various deposition techniques with the primary goal of integrating active thermoelectric materials onto lightweight and flexible substrates for energy conversion. These substrates have showcased their versatility and compatibility with flexible thermoelectric technology, rendering them valuable choices for diverse applications. Further, key deposition methodologies including magnetron sputtering, co-evaporation, spin-coating, and screen printing offer distinct advantages and can be tailored to meet specific material requirements and device designs. These substrates and deposition techniques have shown their versatility and compatibility with flexible thermoelectric technology, rendering them as valuable choices for diverse applications.

References

- [1] Y.Du, J. Xu, B.Paul, P. Eklund. Flexible thermoelectric materials and devices. *Applied Materials Today*(2018), 12, 366-388.
- [2] Q.Jiang, J.Yang, P.Hing, H.Ye. Recent advances, design guidelines, and prospects of flexible organic/inorganic thermoelectric composites. *Materials Advances* (2020), 1(5), 1038-1054.
- [3] R. Mulla, M.H.K Rabinal. Copper sulfides: earth-abundant and low-cost thermoelectric materials. *Energy Technology* (2019), 7(7), 1800850.
- [4] S.Yang, P.Qiu, L.Chen, X.Shi. Recent developments in flexible thermoelectric devices. *Small science* (2021), 1(7), 2100005.
- [5] D.M.Rowe. *Thermoelectrics handbook: macro to nano* (Ed.). (2018). CRC press.
- [6] D.Beretta, N. Neophytou. Thermoelectrics: From history, a window to the future. *Materials Science and Engineering: R: Reports*. (2019), 138, 100501.
- [7] E. Altenkirch, *Phys. Zeitschrift* 12 (1911) 920–924.
- [8] C. Goupil, *Continuum Theory and Modeling of Thermoelectric Elements*, Wiley-VCH Verlag GmbH & Co (2016), Chapter 1, 1-74
- [9] H. J. Goldsmid, R. W. Douglas, *Br. J. Appl. Phys* (1954), 5, 386-390
- [10] G. Slack, *New Materials and Performance Limits for Thermoelectric Cooling*, in: *CRC Handbook of Thermoelectrics*, (ed. D.M. Rowe) CRC Press, 1995.
- [11] A. Shakouri, *Annu. Rev. Mater. Res.* (2011), 41, 399-431.
- [12] L. D. Hicks, M. S. Dresselhaus, *Phys. Rev. B* (1993), 47, 12727-12731.
- [13] C. Kittel, *Introduction to Solid State Physics*, 8. Aufl., Wiley, New York,(2005).
- [14] J.R.Sootsman, D.Y. Chung, M.G.Kanatzidis. New and old concepts in thermoelectric materials. *Angewandte Chemie International Edition* (2009), 48(46), 8616-8639.

- [15] S.Liu, H.Li, P.Li, Y. Liu, C.He. Recent advances in polyaniline-based thermoelectric composites. *CCS Chemistry* (2021), 3(10), 2547-2560.
- [16] C. M. Bhandari, D. M. Rowe, *J. Phys. C* (1978), 11, 1787.
- [17] J.W.Sharp,H.J.Goldsmid,inProc.18thInt. Conf. Thermoelectrics (1999), 709.
- [18] L.Zhang, X.L.Shi, Y.L. Yang, Z.G. Chen. Flexible thermoelectric materials and devices: From materials to applications. *Materials Today* (2021), 46, 62-108.
- [19] Y.Wang, L. Yang, X.L. Shi, X.Shi, L. Chen et al. Flexible thermoelectric materials and generators: challenges and innovations. *Advanced Materials* (2019), 31(29), 1807916.
- [20] Y.Du, S.Z. Shen, K.Cai, P.S.Casey. Research progress on polymer-inorganic thermoelectric nanocomposite materials. *Progress in Polymer Science* (2012), 37(6), 820-841.
- [21] Y.Du, S. Z. Shen,, K. Cai, P.S.Casey. Research progress on polymer-inorganic thermoelectric nanocomposite materials. *Progress in Polymer Science* (2012), 37(6), 820- 841.
- [22] I.Petsagkourakis, K.Tybrandt, X.Crispin ,I. Ohkubo, N. Satoh, T. Mori. Thermoelectric materials and applications for energy harvesting power generation. *Science and technology of advanced materials* (2018), 19(1), 836-862.
- [23] S.N. Patel, M.L.Chabiny. Anisotropies and the thermoelectric properties of semiconducting polymers. *Journal of Applied Polymer Science* (2017), 134(3).
- [24] J. Li, Y. Du, R. Jia, J. Xu,S.Z..Shen. Thermoelectric properties of flexible PEDOT: PSS/polypyrrole/paper nanocomposite films. *Materials* (2017), 10(7), 780.
- [25] Y. Li, Y. Du,Y. Dou, K. Cai, J. Xu, J. PEDOT-based thermoelectric nanocomposites–A mini-review. *Synthetic Metals* (2017), 226, 119-128.
- [26] M. Lay, M. A. Pèlach et al. Smart nanopaper based on cellulose nanofibers with hybrid PEDOT: PSS/polypyrrole for energy storage devices. *Carbohydrate polymers* (2017), 165, 86-95.
- [27] G. H. Kim, L. Shao, K. Zhang, K.P.Pipe. Engineered doping of organic semiconductors for enhanced thermoelectric efficiency. *Nature materials* (2013), 12(8), 719-723.

- [28] K.Sun,S. Zhang, P. Li,Y. Xia, X. Zhang, D. Du,J. Ouyang. Review on application of PEDOTs and PEDOT: PSS in energy conversion and storage devices. *Journal of Materials Science: Materials in Electronics* (2015), 26, 4438-4462.
- [29] L. Stepien, A. Roch, R. Tkachov, T. Gedrange. *Thermoelectrics for Power Generation – A Look at Trends in the Technology*, Intech Open, 2016.
- [30] Y.Du,K.F. Cai,S.Z. Shen, W.D. Yang, P.S. Casey. The thermoelectric performance of carbon black/poly (3, 4-ethylenedioxythiophene): poly (4-styrenesulfonate) composite films. *Journal of Materials Science: Materials in Electronics* (2013), 24, 1702-1706.
- [31] J.Y. Kim,J.H. Jung, D.E.Lee,J. Joo,. Enhancement of electrical conductivity of poly (3, 4-ethylenedioxythiophene)/poly (4-styrenesulfonate) by a change of solvents. *Synthetic Metals* (2002), 126(2-3), 311-316.
- [32] L.Stepien, A.Roch,S. et al. Investigation of the thermoelectric power factor of KOH-treated PEDOT: PSS dispersions for printing applications. *Energy Harvesting and Systems* (2016), 3(1), 101-111.
- [33] Q. Wei, M. Mukaida, Y. Naitoh, T.Ishida. Morphological change and mobility enhancement in PEDOT: PSS by adding co-solvents. *Advanced materials* (2013), 25(20), 2831-2836.
- [34] W. Yuan, J. Cui, Y. Cai, S.Xu. A novel surface modification for calcium sulfate whisker used for reinforcement of poly (vinyl chloride). *Journal of Polymer Research* (2015), 22, 1-9.
- [35] Y. Xia, J.Ouyang. PEDOT: PSS films with significantly enhanced conductivities induced by preferential solvation with cosolvents and their application in polymer photovoltaic cells. *Journal of Materials Chemistry* (2011), 21(13), 4927-4936.
- [36] S. Zhang, Z. Fan, X. Wang, Z.Zhang, J.Ouyang, Enhancement of the thermoelectric properties of PEDOT: PSS via one-step treatment with cosolvents or their solutions of organic salts. *Journal of Materials Chemistry A* (2018), 6(16), 7080-7087.
- [37] H.J. Oh, J.G. Jang, J.-G. Kim, J.-I. Hong, J. Kim, J. Kwak, S.H. Kim, S. Shin, Structural and morphological evolution for water-resistant organic thermoelectrics, *Sci. Rep.* 7 (2017) 1-8.

- [38] Z. Yu, Y. Xia, D. Du, J. Ouyang, PEDOT: PSS films with metallic conductivity through a treatment with common organic solutions of organic salts and their application as a transparent electrode of polymer solar cells, *ACS Appl. Mater. Interfaces* 8 (2016) 11629–11638.
- [39] Z.Fan, D. Du, Z. Yu, P. Li, Y. Xia, J.Ouyang. Significant enhancement in the thermoelectric properties of PEDOT: PSS films through a treatment with organic solutions of inorganic salts. *ACS applied materials & interfaces* (2016), 8(35), 23204–23211.
- [40] N. Kim, S. Kee, S.H. Lee, B.H. Lee, Y.H. Kahng, Y.R. Jo, B.J. Kim, K. Lee, Highly conductive PEDOT:PSS nanofibrils induced by solution-processed crystallization, *Adv. Mater.* 26 (2014) 2268–2272.
- [41] K.C.Chang, M.S.Jeng, C.C. Yang, et al. The thermoelectric performance of poly (3, 4-ethylenedi oxythiophene)/poly (4-styrenesulfonate) thin films. *Journal of electronic materials* (2009), 38, 1182-1188.
- [42] D.A. Mengistie, C.H. Chen, K.M. Boopathi, F.W. Pranoto, L.-J. Li, C.-W. Chu, Enhanced thermoelectric performance of PEDOT:PSS flexible bulky papers by treatment with secondary dopants, *ACS Appl. Mater. Interfaces* 7 (2015) 94–100.
- [43] J. Wang, K. Cai, S. Shen, A facile chemical reduction approach for effectively tuning thermoelectric properties of PEDOT films, *Org. Electron.* 17 (2015) 151–158.
- [44] N. Kim, S. Kee, S.H. Lee, B.H. Lee, Y.H. Kahng, Y.R. Jo, B.J. Kim, K. Lee, Highly conductive PEDOT: PSS nanofibrils induced by solution-processed crystallization, *Adv. Mater.* 26 (2014) 2268–2272.
- [45] M. Culebras, C. Gomez, ´ A. Cantarero, Enhanced thermoelectric performance of PEDOT with different counter-ions optimized by chemical reduction, *J. Mater. Chem. A* 2 (2014) 10109–10115.
- [46] J. J. Luo, D. Billep, T. Waechtler, T. Otto, M. Toader, O. Gordan, E. Sheremet, J. Martin, M. Hietschold, D. R. T. Zahnd, and T. Gessner, Enhancement of the thermoelectric properties of PEDOT:PSS thin films by post-treatment, *J. Mater. Chem. A* (2013), 1, 7576.

- [47] G. H. Kim, L. Shao, K. Zhang, and K. P. Pipe, Engineered doping of organic semiconductors for enhanced thermoelectric efficiency, *Nat. Mater* (2013), 12, 719.
- [48] S. Lee, S. Kim, A. Pathak, A. Tripathi et al. Recent progress in organic thermoelectric materials and devices. *Macromolecular Research* (2020), 28(6), 531-552.
- [49] O. Bubnova, M. Berggren, X. Crispin, Tuning the thermoelectric properties of conducting polymers in an electrochemical transistor, *JACS* 134 (2012) 16456-16459.
- [50] S.H. Lee, H. Park, W. Son, H.H. Choi, J.H. Kim, Novel solution-processable, dedoped semiconductors for application in thermoelectric devices, *J. Mater. Chem. A* 2 (2014) 13380-13387.
- [51] H. Park, S.H. Lee, F.S. Kim, H.H. Choi, I.W. Cheong, J.H. Kim, Enhanced thermoelectric properties of PEDOT: PSS nanofilms by a chemical dedoping process, *J. Mater. Chem. A* 2 (2014) 6532-6539.
- [52] N. Massonnet, A. Carella, O. Jaudouin, P. Rannou, G. Laval, C. Celle, J.- P. Simonato, Improvement of the Seebeck coefficient of PEDOT: PSS by chemical reduction combined with a novel method for its transfer using free-standing thin films, *J. Mater. Chem. C* 2 (2014) 1278-1283.
- [53] L. Zhang, H. Deng, S. Liu, Q. Zhang, F. Chen, Q. Fu, Enhanced thermoelectric properties of PEDOT: PSS films via a novel two-step treatment, *RSC Adv.* 5 (2015) 105592-105599.
- [54] J. Luo, D. Billep, T. Waechtler, T. Otto, M. Toader, O. Gordan, E. Sheremet, J. Martin, M. Hietschold, D.R. Zahn, Enhancement of the thermoelectric properties of PEDOT: PSS thin films by post-treatment, *J. Mater. Chem. A* 1 (2013) 7576-7583.
- [55] T.C. Tsai, H.C. Chang, C.H. Chen, Y.C. Huang, W.T. Whang, A facile dedoping approach for effectively tuning thermoelectricity and acidity of PEDOT: PSS films, *Org. Electron.* 15 (2014) 641-645.
- [56] E. Yang, J. Kim, B.J. Jung, J. Kwak, Enhanced thermoelectric properties of sorbitol-mixed PEDOT: PSS thin films by chemical reduction, *J. Mater. Sci.: Mater. Electron* 26 (2015) 2838-2843.
- [57] Z. Zhu, C. Liu, H. Shi, Q. Jiang, J. Xu, F. Jiang, J. Xiong, E. Liu, An effective approach to enhanced thermoelectric properties of

- PEDOT: PSS films by a DES post-treatment, *J. Polym. Sci., Part B: Polym. Phys.* 53 (2015) 885–892.
- [58] S.H. Lee, H. Park, S. Kim, W. Son, I.W. Cheong, J.H. Kim, Transparent and flexible organic semiconductor nanofilms with enhanced thermoelectric efficiency, *J. Mater. Chem. A.* 2(2014) 7288–7294.
- [59] J. Kim, J.G. Jang, J.-I. Hong, S.H. Kim, J. Kwak, Sulfuric acid vapor treatment for enhancing the thermoelectric properties of PEDOT: PSS thin-films, *J. Mater. Sci.: Mater. Electron.* 27 (2016) 6122– 6127.
- [60] Z. Fan, D.H. Du, H.Y. Yao, J.Y. Ouyang, Higher PEDOT molecular weight giving rise to higher thermoelectric property of PEDOT:PSS: a comparative study of clevios P and Clevios PH1000, *ACS Appl. Mater. Interfaces* 9 (2017) 11732–11738.
- [61] Z.Fan,D.Du, X. Guan, J.Ouyang. Polymer films with ultrahigh thermoelectric properties arising from significant seebeck coefficient enhancement by ion accumulation on surface. *Nano energy*, 51 (2018), 481-488.
- [62] Z. Fan, D. Du, Z. Yu, P. Li, Y. Xia, J. Ouyang, Significant enhancement in the thermoelectric properties of PEDOT:PSS films through a treatment with organic solutions of inorganic salts, *ACS Appl. Mater. Interfaces* 8 (2016) 23204–23211.
- [63] C. Yi, A. Wilhite, L. Zhang, R. Hu, S. S. Chuang, J. Zheng, and X. Gong, *ACS Appl. Mater. Interfaces* (2015), 7, 8984.
- [64] O. Bubnova, Z. U. Khan, A. Malti, S. Braun, M. Fahlman, M. Berggren, and X. Crispin, *Nat. Mater*, 10(2011), 429.
- [65] T. Park, C. Park, B. Kim, H. Shin, and E. Kim, Flexible PEDOT electrodes with large thermoelectric power factors to generate electricity by the touch of fingertips, *Energy Environ. Sci* 6(2013),, 788.
- [66] F.Yakuphanoglu, B.F.Senkal. Thermoelectrical and Optical Properties of Double Wall Carbon Nanotubes:Polyaniline Containing Boron n-Type Organic Semiconductors. *Polym. Adv. Technol.*, 19 (2008), 905–908.
- [67] K.Chatterjee, M.Mitra, K. Kargupta, S. Ganguly, D. Banerjee. Synthesis Characterization and Enhanced Thermoelectric Performance of Structurally Ordered Cable-like Novel

- Polyaniline-Bismuth Telluride Nanocomposite. *Nanotechnology*, 24 (2013), 215703.
- [68] M.Mitra, C.Kulsi, K.Chatterjee, K. Kargupta, S.Ganguly, D. Banerjee, S.Goswami. Reduced Graphene Oxide-Polyaniline Composites – Synthesis, Characterization and Optimization for Thermoelectric Applications. *RSC Adv*, 5 (2015), 31039–31048.
- [69] M.J. Chatterjee, D.Banerjee, K. Chatterjee. Composite of Single Walled Carbon Nanotube and Sulfosalicylic Acid Doped Polyaniline: A Thermoelectric Material. *Mater. Res. Express*, 3 (2016), 085009.
- [70] S. Yun, Y. Qin, A.R. Uhl, N. Vlachopoulos, M. Yin, D. Li, X. Han, A. Hagfeldt, New generation integrated devices based on dye-sensitized and perovskite solar cells, *Energy Environ. Sci.* 11 (2018) 476–526.
- [71] R. Chan Yu King, F.Roussel, J.F.Brun, C.Gors. Carbon Nanotube-Polyaniline Nanohybrids: Influence of the Carbon Nanotube Characteristics on the Morphological, Spectroscopic, Electrical and Thermoelectric Properties. *Synth. Met*, 162 (2012), 1348–1356.
- [72] Y.Zhao, G.S. Tang, Z.Z. Yu, J.S. Qi. The Effect of Graphite Oxide on the Thermoelectric Properties of Polyaniline. *Carbon*, 50 (2012), 3064–3073.
- [73] J.Xiang, L.T.Drzal. Templated Growth of Polyaniline on Exfoliated Graphene Nanoplatelets (GNP) and Its Thermoelectric Properties. *Polymer*, 53 (2012), 4202–4210.
- [74] Y.Du, S.Z.Shen, W.Yang. Donelson, R.; Cai, K.; Casey, P. S. Simultaneous Increase in Conductivity and Seebeck Coefficient in a Polyaniline/Graphene Nanosheets Thermoelectric Nanocomposite. *Synth. Met.*, 161 (2012), 2688–2692.
- [75] M.Cochet, W.K.Maser, A.M. Benito, M.A.Callejas, M.T.Martínez, J.M.Benoit, J.Schreiber, O.Chauvet. Synthesis of a New Polyaniline/Nanotube Composite: “In-Situ” Polymerisation and Charge Transfer through Site-Selective Interaction. *Chem. Comm.* (2001), 1450–1451.
- [76] H.Zengin, W.Zhou, J. Jin, R. Czerw, D.W. Smith, L.Echegoyen, D.L. Carroll, S.H.Foulger, J.Ballat. Carbon Nanotube Doped Polyaniline. *Adv. Mater*, 14 (2002), 1480–1483.

- [77] M. Baibarac, I. Baltog, S. Lefrant, J. Mevellec, O. Chauvet. Polyaniline and Carbon Nanotubes Based Composites Containing Whole Units and Fragments of Nanotubes. *Chem. Mater.*, 15 (2003), 4149- 4156.
- [78] H. Wang, L. Yin, X. Pu, C. Yu. Facile Charge Carrier Adjustment for Improving Thermopower of Doped Polyaniline. *Polymer*, 54 (2013), 1136-1140.
- [79] Y.Cao, P.Smith. Liquid-Crystalline Solutions of Electrically Conducting Polyaniline. *Polymer*, 34 (1993), 3139-3143.
- [80] Y.Cao, P.Smith, A.J.Heeger. Counter-Ion Induced Processibility of Conducting Polyaniline and of Conducting Polyblends of Polyaniline in Bulk Polymers. *Synth. Met.*, 48 (1992), 91-97.
- [81] Y.Cao, A.J.Heeger. Magnetic Susceptibility of Polyaniline in Solution in Non-Polar Organic Solvents and in Polyblends in Poly(methyl methacrylate). *Synth. Met.*, 52 (1992), 193-200.
- [82] A.G.MacDiarmid, A.J.Epstein,. Secondary Doping in Polyaniline. *Synth. Met.*, 69 (1995), 85-92.
- [83] A. MacDiarmid, A. J.Epstein. The Concept of Secondary Doping as Applied to Polyaniline. *Synth. Met.*, 65 (1994), 103-116.
- [84] O. T. Ikkala, L. O.Pietilä, L.Ahjopalo, H.Österholm, P. J. Passiniemi. On the Molecular Recognition and Associations between Electrically Conducting Polyaniline and Solvents. *J. Chem. Phys.*, 103 (1995), 9855-9863.
- [85] Q.Yao, Q.Wang, L. Wang, Y.Wang, J.Sun, H.Zeng, Z.Jin, X.Huang, L .Chen. The Synergic Regulation of Conductivity and Seebeck Coefficient in Pure Polyaniline by Chemically Changing the Ordered Degree of Molecular Chains. *J. Mater. Chem. A*, 2 (2014), 2634-2640.
- [86] C. Nath, A. Kumar, Y.-K. Kuo, G.S. Okram, High thermoelectric figure of merit in nanocrystalline polyaniline at low temperatures, *Appl. Phys. Lett.* 105 (2014), 133108.
- [87] H. Yan, N. Toshima, Thermoelectric properties of alternatively layered films of polyaniline and (\pm)-10-camphorsulfonic acid-doped polyaniline, *Chem. Lett.* 28 (1999) 1217-1218.
- [88] S. Wakim, B.R. Aïch, Y. Tao, M. Leclerc, Charge transport, photovoltaic, and thermoelectric properties of poly (2, 7-carbazole) and poly (indolo [3, 2-b] carbazole) derivatives, *Polym. Rev.* 48 (2008) 432-462.

- [89] I. L'evesque, X. Gao, D.D. Klug, S.T. John, C.I. Ratcliffe, M. Leclerc, Highly soluble poly (2, 7-carbazolenevinylene) for thermoelectrical applications: From theory to experiment, *React. Funct. Polym.* 65 (2005) 23–36.
- [90] I. L'evesque, P.-O. Bertrand, N. Blouin, M. Leclerc, S. Zecchin, G. Zotti, C. I. Ratcliffe, D.D. Klug, X. Gao, F. Gao, Synthesis and thermoelectric properties of polycarbazole, polyindolocarbazole, and polydiindolocarbazole derivatives, *Chem. Mater.* 19 (2007) 2128–2138.
- [91] R.B. Aïch, N. Blouin, A. Bouchard, M. Leclerc, Electrical and thermoelectric properties of poly (2, 7-carbazole) derivatives, *Chem. Mater.* 21 (2009) 751–757.
- [92] Y. Xuan, X. Liu, S. Desbief, P. Leclerc, M. Fahlman, R. Lazzaroni, M. Berggren, J. Cornil, D. Emin, X. Crispin, Thermoelectric properties of conducting polymers: the case of poly (3-hexylthiophene), *Phys. Rev. B: Condens. Matter* 82 (2010), 115454.
- [93] Q. Zhang, Y. Sun, W. Xu, D. Zhu, Thermoelectric energy from flexible P3HT films doped with a ferric salt of triflimide anions, *Energy Environ. Sci.* 5 (2012) 9639–9644.
- [94] S. Qu, Q. Yao, L. Wang, Z. Chen, K. Xu, H. Zeng, W. Shi, T. Zhang, C. Uher, L. Chen, Highly anisotropic P3HT films with enhanced thermoelectric performance via organic small molecule epitaxy, *e292*, *NPG Asia Mater.* 8 (2016).
- [95] N. Basescu, Z.-X. Liu, D. Moses, A. Heeger, H. Naarmann, N. Theophilou, High electrical conductivity in doped polyacetylene, *Nat* 327 (1987) 403–405.
- [96] H. Kaneko, T. Ishiguro, A. Takahashi, J. Tsukamoto, Magnetoresistance and thermoelectric power studies of metal-nonmetal transition in iodine-doped polyacetylene, *Synth. Met.* 57 (1993) 4900–4905.
- [97] R. Zuzok, A. Kaiser, W. Pukacki, S. Roth, Thermoelectric power and conductivity of iodine-doped “new” polyacetylene, *J. Chem. Phys.* 95 (1991) 1270–1275.
- [98] Y. Du, K. F. Cai, S. Z. Shen, B. An, Z. Qin, P. S. Casey. Influence of sintering temperature on thermoelectric properties of Bi₂Te₃/Polythiophene composite materials. *Journal of Materials Science: Materials in Electronics*, 23 (2012), 870-876.

- [99] J.Xiong, L.Wang, J.Xu, C.Liu, W.Zhou, H.Shi et al. Thermoelectric performance of PEDOT: PSS/Bi₂Te₃-nanowires: a comparison of hybrid types. *Journal of Materials Science: Materials in Electronics*, 27(2016), 1769-1776.
- [100] Y.Du, K.F. Cai, S.Chen, P. Cizek, T. Lin. Facile preparation and thermoelectric properties of Bi₂Te₃ based alloy nanosheet/PEDOT: PSS composite films. *ACS applied materials & interfaces* (2014)., 6(8), 5735-5743.
- [101] T. Zhang., K.Li, C. Li, S. Ma, H.H. Hng, L.Wei. Mechanically durable and flexible thermoelectric films from PEDOT: PSS/PVA/Bi_{0.5}Sb_{1.5}Te₃ nanocomposites. *Advanced Electronic Materials* (2017). 3(4), 1600554.
- [102] K. C. See, J.P. Feser, C.E. Chen, A. Majumdar, J.J. Urban, R.A. Segalman. Water-processable polymer– nanocrystal hybrids for thermoelectrics. *Nano letters* (2010), 10(11), 4664-4667.
- [103] H.Song, K.Cai, S. Shen. Enhanced thermoelectric properties of PEDOT/PSS/Te composite films treated with H₂SO₄. *Journal of Nanoparticle Research* (2016), 18, 1-9.
- [104] H.Song, K.Cai. Preparation and properties of PEDOT: PSS/Te nanorod composite films for flexible thermoelectric power generator. *Energy* (2017), 125, 519-525.
- [105] R.Tian, C.Wan et al. A solution-processed TiS₂/organic hybrid superlattice film towards flexible thermoelectric devices. *Journal of Materials Chemistry A* (2017), 5(2), 564-570.
- [106] C.Wan, R.Tian, M. Kondou, R.Yang, P. Zong, P. K. Koumoto, Ultrahigh thermoelectric power factor in flexible hybrid inorganic-organic superlattice. *Nature communications*(2017), 8(1), 1024.
- [107] C.Wan, X. Gu, F. Dang, T.Itoh, Y.Wang, H.Sasaki et al. Flexible n-type thermoelectric materials by organic intercalation of layered transition metal dichalcogenide TiS₂. *Nature materials* (2015), 14(6), 622-627.
- [108] C.Jiang, P. Wei, Y.Ding, K.Cai, L.Tong, L et al. Ultrahigh performance polyvinylpyrrolidone/Ag₂Se composite thermoelectric film for flexible energy harvesting. *Nano Energy* (2021), 80, 105488.

- [109] Y.Chen, M.He, B. Liu, G.C. Bazan, J.Zhou, Z.Liang. Bendable n-type metallic nanocomposites with large thermoelectric power factor. *Advanced Materials* (2017), 29(4), 1604752.
- [110] C.Zhou, C. Dun, Q. Wang, K.Wang, K, Z.Shi, D.L.Carroll et al. Nanowires as building blocks to fabricate flexible thermoelectric fabric: the case of copper telluride nanowires. *ACS Applied Materials & Interfaces* (2015), 7(38), 21015-21020.
- [111] J.S.Yun, S.Choi, S.H.Im. Advances in carbon-based thermoelectric materials for high-performance, flexible thermoelectric devices. *Carbon Energy* (2021). 3(5), 667-708.
- [112] S.L.Kim, K.Choi, A. Tazebay, C.Yu. Flexible power fabrics made of carbon nanotubes for harvesting thermoelectricity. *ACS Nano* (2014), 8(3), 2377-2386.
- [113] An CJ, Kang YH, Song H, Jeong Y, Cho SY. High-performance flexible thermoelectric generator by control of electronic structure of directly spun carbon nanotube webs with various molecular dopants. *J Mater Chem A*. (2017), (30):15631-15639
- [114] M.L.Wu, Y. Chen, L. Zhang, H. Zhan, L.Qiang, J.N.Wang. High-performance carbon nanotube/polymer composite fiber from layer-by-layer deposition. *ACS applied materials & interfaces* (2016), 8(12), 8137-8144.
- [115] S.Qu, M.Wang, Y.Chen, Q.Yao, L.Chen. Enhanced thermoelectric performance of CNT/P3HT composites with low CNT content. *RSC advances* (2018), 8(59), 33855-33863.
- [116] Q.Yao, Q.Wang, L.Wang, L. Chen. Abnormally enhanced thermoelectric transport properties of SWNT/PANI hybrid films by the strengthened PANI molecular ordering. *Energy & Environmental Science* (2014), 7(11), 3801-3807.
- [117] Y.Chen, S.Qu, W.Shi, Q.Yao, L.Chen. Enhanced thermoelectric properties of copper phthalocyanine/single-walled carbon nanotubes hybrids. *Carbon* (2020), 159, 471-477.
- [118] B.Chen, M.Kruse, B.Xu, R.Tutika, W.Zheng et al. Flexible thermoelectric generators with inkjet-printed bismuth telluride nanowires and liquid metal contacts. *Nanoscale*(2019), 11(12), 5222-5230.
- [119] D.Ding, F.Sun, F.Xia, Z.Tang. A high-performance and flexible thermoelectric generator based on the solution-processed composites of reduced graphene oxide nanosheets and bismuth

- telluride nanoplates. *Nanoscale Advances* (2020), 2(8), 3244-3251.
- [120] M.M.Mallick, A.G. Rösch, L.Franke, S.Ahmed, A.Gall, H.Geißwein et al. High-performance Ag–Se-based n-type printed thermoelectric materials for high-power density folded generators. *ACS applied materials & interfaces* (2020), 12(17), 19655-19663.
- [121] S.Yang, K.Cho, J.Yun, J.Choi, S.Kim. Thermoelectric characteristics of γ -Ag₂Te nanoparticle thin films on flexible substrates. *Thin Solid Films* (2017), 641, 65-68.
- [122] M.Saeidi-Javash, W. Kuang, C. Dun, Y.Zhang. 3D conformal printing and photonic sintering of high-performance flexible thermoelectric films using 2D nanoplates. *Advanced Functional Materials*(2019), 29(35), 1901930.
- [123] S.Ferhat, C.Domain, J.Vidal, D.Noël, B.Ratier, B.Lucas. Flexible thermoelectric device based on TiS₂ (HA) x n-type nanocomposite printed on paper. *Organic Electronics* (2019), 68, 256-263.
- [124] S.J.Kim, H.E.Lee, H.Choi, Y. Kim, J.H.We, J.S. Shin et al. High-performance flexible thermoelectric power generator using laser multiscanning lift-off process. *ACS nano* (2016), 10(12), 10851-10857.
- [125] Huang, X.; Deng, L.; Liu, F.; Zhang, Q.; Chen, G. Effect of Crystalline Microstructure Evolution on Thermoelectric Performance of PEDOT: PSS Films. *Energy Mater. Adv.* 2021, 2021, 1–10
- [126] Yang, J.; Jia, Y.; Liu, Y.; Liu, P.; Wang, Y.; Li, M.; Jiang, F.; Lan, X.; Xu, J. PEDOT:PSS/PVA/Te ternary composite fibers toward flexible thermoelectric generator. *Compos. Commun.* 2021, 27, 100855.
- [127] S. Gogoc, Przemyslaw Data. Organic thermoelectric materials as the waste heat remedy, *Molecules*, 3 (2022), 1016.
- [128] Y. Lu, Li, X., Cai, K., Gao, M., Zhao, W., He, J., & Wei, P. Enhanced-performance PEDOT: PSS/Cu₂Se-based composite films for wearable thermoelectric power generators. *ACS Applied Materials & Interfaces*, 13(2021), 631-638.
- [129] H. J. Ahn, Kim, S., Kim, K. H., Lee, J. Y. Preparation and characterization of thermoelectric PEDOT/Te nanorod array composite films. *Materials*, 15(2022), 148.

- [130] L. Jin, Y. Hao, et al., Tellurium/polymers for flexible thermoelectrics: status and challenges. *Journal of Materials Chemistry A*, (2023).
- [131] Du J., Zhang B., Jiang M., Zhang Q., Zhang K., Liu, et al. Inkjet Printing Flexible Thermoelectric Devices Using Metal Chalcogenide Nanowires. *Advanced Functional Materials*, (2023), 2213564.
- [132] Wu Q., Zha K., Zhang J., Zhang J, et al., SnS/PEDOT: PSS composite films with enhanced surface conductivities induced by solution post-treatment and their application in flexible thermoelectric. *Organic Electronics*, 118(2023), 106799.
- [133] Bounioux, C., Díaz-Chao, P., Campoy-Quiles, M., Martín-González, M. S., Goni, A. R., Yerushalmi-Rozen, Müller, C. Thermoelectric composites of poly (3-hexylthiophene) and carbon nanotubes with a large power factor. *Energy & Environmental Science*, 6(2013), 918-925.
- [134] Hwang, H., & Jang, K. S. (2021). Thermoelectric all-carbon heterostructures for a flexible thermoelectric generator. *Sustainable Energy & Fuels*, 5(1), 267-273.
- [135] An, C. J., Kang, Y. H., Song, H., Jeong, Y., & Cho, S. Y. High-performance flexible thermoelectric generator by control of electronic structure of directly spun carbon nanotube webs with various molecular dopants. *Journal of materials Chemistry A*, 5(2017), 15631-15639.
- [136] Yin, X., Peng, Y., Luo, J., Zhou, X., Gao, C., Wang, L., & Yang, C. Tailoring the framework of organic small molecule semiconductors towards high-performance thermoelectric composites via conglutinated carbon nanotube webs. *Journal of Materials Chemistry A*, 6(2018), 8323-8330.